

1 **Mapping eQTLs With RNA-Seq Reveals Novel SLE Susceptibility Genes, Non-Coding**
2 **RNAs, and Alternative-Splicing Events That Are Concealed Using Microarrays**

3

4 Christopher A. Odhams^{1*}, Andrea Cortini¹, Lingyan Chen¹, Amy L. Roberts¹, Ana Vinuela⁴,
5 Alfonso Buil²⁻³, Kerrin S. Small⁴, Emmanouil T. Dermitzakis²⁻³, David L. Morris¹, Timothy J.
6 Vyse^{1,5*}, Deborah S. Cunninghame Graham^{*1,5}

7

8 ¹Division of Genetics and Molecular Medicine, King's College London, London, SE1 9RT,
9 UK. ²Department of Genetic Medicine and Development, University of Geneva Medical
10 School, Geneva, CH – 1211 Geneva 4, Switzerland.

11 ³Institute of Genetics and Genomics in Geneva, University of Geneva, Geneva, CH – 1211
12 Geneva 4 Switzerland.

13 ⁴Department of Twin Research and Genetic Epidemiology, King's College London, London,
14 SE1 7EH, UK.

15 ⁵Division of Immunology, Infection and Inflammatory Disease, King's College London,
16 London, SE1 1UL, UK.

17

18 *Correspondence: Dr Deborah S. Cunninghame Graham

19 Fax: +44 (0)207 188 2585

20 Telephone: +44 (0)207 848 8504

21 Email: deborah.cunninghame-graham@kcl.ac.uk

22 **Abstract**

23 Studies attempting to functionally interpret complex-disease susceptibility loci by GWAS and
24 eQTL integration have predominantly employed microarrays to quantify gene-expression.
25 RNA-Seq has the potential to discover a more comprehensive set of eQTLs and illuminate
26 the underlying molecular consequence. We examine the functional outcome of 39 variants
27 associated with Systemic Lupus Erythematosus (SLE) through integration of GWAS and
28 eQTL data from the TwinsUK microarray and RNA-Seq cohort in lymphoblastoid cell lines.
29 We use conditional analysis and a Bayesian colocalisation method to provide evidence of a
30 shared causal-variant, then compare the ability of each quantification type to detect disease
31 relevant eQTLs and eGenes. We discovered a greater frequency of candidate-causal eQTLs
32 using RNA-Seq, and identified novel SLE susceptibility genes that were concealed using
33 microarrays (e.g. *NADSYN1*, *SKP1*, and *TCF7*). Many of these eQTLs were found to
34 influence the expression of several genes, suggesting risk haplotypes may harbour multiple
35 functional effects. We pinpointed eQTLs modulating expression of four non-coding RNAs;
36 three of which were replicated in whole-blood. Novel SLE associated splicing events were
37 identified in the T-reg restricted transcription factor, *IKZF2*, the autophagy-related gene
38 *WDFY4*, and the redox coenzyme *NADSYN1*, through asQTL mapping using the Geuvadis
39 cohort. We have significantly increased our understanding of the genetic control of gene-
40 expression in SLE by maximising the leverage of RNA-Seq and performing integrative
41 GWAS-eQTL analysis against gene, exon, and splice-junction quantifications. In doing so,
42 we have identified novel SLE candidate genes and specific molecular mechanisms that will
43 serve as the basis for targeted follow-up studies.

44 **Introduction**

45 Genome-Wide Association Studies (GWAS) have successfully identified a large number of
46 genetic loci that contribute to complex-disease susceptibility in humans (1). Evidence
47 suggests these variants are enriched within regulatory elements of the genome and their
48 effects play a central role in modulation of intermediate quantitative phenotypes such gene
49 expression (1–6). Many expression quantitative trait loci (eQTL) mapping studies have since
50 been conducted across a wide-range of ethnicities (7, 8), cell-types (9–16), disease states
51 (17–22) and in response to various environmental stimuli (23, 24) - with each contributing to
52 our understanding of the architecture of human regulatory variation in complex-disease.

53

54 In spite of diverse study designs, a significant constraint on the majority of such
55 investigations is the use of 3'-targeted microarrays to profile gene expression. The effects of
56 splicing are less likely to be detected through quantification of pre-defined probes that target
57 common exons of a gene (25) and may explain why only a limited number of susceptibility
58 loci localize to causal eQTL signals (26, 27). Technical limitations of microarrays and noise
59 from the small probe design of exon-arrays, further hinder the accuracy of expression
60 measurements (25, 28–30). RNA-Seq based eQTL mapping studies are beginning to
61 emerge (31, 32) and, although large-scale analysis pipelines are still being streamlined, such
62 types of investigations will greatly increase the likelihood of capturing disease associated
63 eQTLs as quantification of overall gene and independent exon expression, and relative
64 transcript abundance (including novel isoforms and non-coding RNAs) is possible (33–39).

65

66 Integrative studies using RNA-Seq to functionally annotate complex-disease susceptibility
67 loci however have been limited (35, 40–44). Moreover, numerous investigations have aimed
68 to explain the functional relevance of susceptibility loci by interrogation of GWAS SNPs
69 themselves in eQTL datasets and simply testing for association with gene expression (45–
70 47). Such inferential observations should be treated with caution as they may possibly be the

71 result of coincidental overlap between disease association and eQTL signal due to local LD
72 and general ubiquity of regulatory variants (48). This has become particularly important as
73 statistical power in eQTL cohorts grow and availability of summary-level data accession
74 through eQTL data-browsers increases (49–51).

75

76 In this investigation, we integrate eQTL data derived from both microarray and RNA-Seq
77 experiments with our GWAS results in Systemic Lupus Erythematosus (SLE [MIM: 152700]);
78 a heritable autoimmune disease with undefined aetiology and over 50 genetically associated
79 loci (52–54). We use summary-level *cis*-eQTL results in lymphoblastoid cell lines (LCLs)
80 taken from the TwinsUK cohort to directly compare the microarray (9) and RNA-Seq (39)
81 results in detecting SLE associated eQTLs along with their accompanying eGenes. We
82 apply a rigorous two-step approach – a combination of conditional (55) and Bayesian
83 colocalisation (56) analysis – to test for a shared causal variant at each locus. We
84 demonstrate the benefits of using RNA-Seq over microarrays in eQTL analysis by identifying
85 not only novel SLE candidate-causal eGenes but also putative molecular mechanisms by
86 which SLE-associated SNPs may act; including differential exon usage, and expression
87 modulation of non-coding RNA. Our investigation was extended to include RNA-Seq
88 expression data in whole blood in order to validate the eQTL signals detected in LCLs and
89 uncover the differences in genetic control of expression between cell-types. Finally, we
90 interrogate the Geuvadis RNA-Seq cohort (35) to identify SLE associated alternative-splicing
91 quantitative trait loci (asQTLs) and highlight the advantages of profiling at various resolutions
92 to detect eQTLs that would otherwise remain concealed. Through functional annotation of
93 SLE associated loci using microarray and RNA-Seq derived expression data, we have
94 supplied comprehensive evidence of the need to use RNA-Seq to detect disease
95 contributing eQTLs and, in doing so, have suggested novel functional mechanisms that
96 serve as a basis for future targeted follow-up studies.

97 **Results**

98 **Discovery and classification of SLE candidate-causal eQTLs and eGenes**

99 The first part of this study integrated the 39 SLE associated SNPs taken from a recent
100 GWAS in Europeans (**Table 1**) with eQTLs from the TwinsUK gene-expression cohort
101 (n=856) profiled using microarray and RNA-Seq (at both gene-level and exon-level
102 resolutions). To accomplish this, we implemented a two-step pipeline (**Fig. 1**), and subjected
103 the genomic intervals within +/-1Mb of each of the 39 GWAS SNPs to eQTL association
104 analysis against expression quantifications in LCLs (**Table 2**).

105

106 Full results of the conditional and colocalisation analysis for each significant association are
107 presented in **S1 Table**, **S2 Table**, and **S3 Table** for microarray, RNA-Seq (gene-level), and
108 RNA-Seq (exon-level), respectively. Statistically significant SLE-associated *cis*-eQTLs
109 showing evidence of a shared causal variant or in very strong LD and close ranking between
110 the disease and *cis*-eQTL signal following conditional and colocalisation analyses were
111 classified as SLE candidate-causal eQTLs as stated in Methods. SLE candidate-causal
112 eGenes were defined as genes whose expression is modulated by the eQTL. The final
113 column of **S1-S3 Tables** indicates whether each GWAS SNP is deemed to be candidate-
114 causal. These SLE candidate-causal eQTLs and eGenes are presented in separate tables
115 contingent on the dataset from which they were generated: results from microarray
116 assessment are listed in **Table 3**, from RNA-Seq (gene-level) in **Table 4**, and from RNA-Seq
117 (exon-level) in **Table 5**. Effect sizes are with respect to the minor allele; risk alleles are
118 highlighted in **Table 1**. Overall, exon-level analysis was the most effective quantification type
119 for the discovery of eQTLs and eGenes compared with gene-level RNA-Seq or microarray
120 analysis following an FDR cut-off of $q < 0.05$ and conditional and colocalisation thresholding
121 as described.

Table 1
Independent allelic associations at SLE susceptibility loci following meta-analysis with replication study

GWAS SNP (Tag SNP)	GWAS SNP Position (hg19)	Variant Alleles	Odds Ratio (CI)	P-value	GENCODE v10 Annotation	Annotated eGenes from microarray LCLs
rs2476601	1:114377568	G/A	1.43 (1.34-1.53)	1.10E-28	<i>PTPN22</i> Missense	
rs1801274	1:161479745	G/A	1.16 (1.11-1.21)	1.04E-12	<i>FCGR2A</i> Missense	<i>FCGR2B</i>
rs10912578 (rs844663)	1:173251856	G/A	1.27 (1.22-1.33)	4.16E-19	<i>LOC100506023</i> Intronic	
rs10753074 (rs1935325)	1:173346343	T/C	1.21 (1.15-1.26)	5.82E-12	<i>LOC100506023</i> Intronic	
rs17849501	1:183542323	C/T	2.10 (1.95-2.26)	3.45E-88	<i>NCF2</i> Synonymous	<i>SMG7</i>
rs3024505	1:206939904	G/A	1.17 (1.11-1.24)	4.64E-09	1kb 3' of <i>IL10</i>	
rs9782955	1:236039877	C/T	1.16 (1.11-1.22)	1.25E-09	<i>LYST</i> Intronic	<i>LYST</i>
rs268134	2:65608363	G/A	1.21 (1.15-1.27)	1.14E-10	<i>SPRED</i> Intronic	<i>SPRED2</i>
rs2111485	2:163110536	G/A	1.15 (1.11-1.2)	1.27E-11	8.9kb 5' of <i>FAP</i>	
rs11889341	2:191943742	C/T	1.70 (1.64-1.75)	2.48E-75	<i>STAT4</i> Intronic	
rs6736175 (rs16833249)	2:191946322	T/C	1.24 (1.19-1.29)	9.17E-17	<i>STAT4</i> Intronic	
rs3768792	2:213871709	A/G	1.24 (1.17-1.31)	1.21E-13	<i>IKZF2</i> 3'-UTR	
rs9311676 (rs11714389)	3:58470351	C/T	1.17 (1.13-1.22)	3.06E-14	<i>LOC101929223</i> NC	<i>ABHD6</i>
rs564799	3:159728987	C/T	1.14 (1.09-1.18)	1.54E-09	<i>IL12A-AS1</i> Intronic	<i>IL12A</i>
rs10028805	4:102737250	G/A	1.20 (1.15-1.25)	4.31E-17	<i>BANK1</i> Intronic	<i>BANK1</i>
rs7726414 (rs17167273)	5:133431834	C/T	1.45 (1.32-1.58)	4.44E-16	19kb 5' of <i>TCF7</i>	
rs10036748	5:150458146	C/T	1.38 (1.32-1.45)	1.27E-45	<i>TNIP1</i> Intronic	
rs2431697	5:159879978	T/C	1.26 (1.21-1.31)	8.01E-28	15kb 5' of <i>hsa-mir-146a</i>	
rs6568431	6:106588806	C/A	1.21 (1.15-1.27)	5.04E-14	31kb 3' of <i>PRDM1</i>	
rs6932056	6:138242437	T/C	1.83 (1.65-2.02)	1.97E-31	22kb 3' of <i>RP11-10J5.1</i>	
rs849142	7:28185891	T/C	1.14 (1.1-1.19)	8.61E-11	<i>JAZF1</i> Intronic	
rs4917014	7:50305863	T/G	1.18 (1.13-1.24)	6.39E-14	8.5kb 3' of <i>AC020743.4</i>	
rs3757387 (rs4728142)	7:128576086	T/C	1.45 (1.4-1.5)	1.14E-48	1.6kb 5' of <i>IRF5</i>	
rs35000415 (rs10488631)	7:128585616	C/T	1.83 (1.76-1.9)	1.20E-60	<i>IRF5</i> Intronic	<i>IRF5, TNPO3</i>
rs2736340	8:11343973	C/T	1.29 (1.22-1.37)	6.28E-20	7.5kb 5' of <i>BLK</i>	<i>BLK</i>
rs2663052	10:50069395	G/A	1.16 (1.1-1.22)	5.25E-09	<i>WDFY4</i> Intronic	<i>WDFY4</i>
rs4948496	10:63805617	T/C	1.14 (1.1-1.19)	1.04E-10	<i>ARID5B</i> Intronic	
rs12802200 (rs2396545)	11:566936	C/A	1.23 (1.15-1.31)	8.81E-10	<i>MIR210HG</i> NC	
rs2732549	11:35088399	A/G	1.24 (1.19-1.29)	1.20E-23	46kb 3' of <i>PDHX</i>	
rs3794060	11:71187679	T/C	1.23 (1.18-1.29)	1.32E-20	<i>NADSYN1</i> Intronic	
rs7941765 (rs6590343)	11:128499000	C/T	1.14 (1.1-1.19)	1.35E-10	547bp 3' of <i>RP11-744N12.3</i>	
rs10774625	12:111910219	A/G	1.13 (1.08 - 1.18)	4.09E-09	<i>ATXN2</i> Intronic	
rs1059312	12:129278864	A/G	1.17 (1.12-1.21)	1.48E-13	<i>SLC15A4</i> Synonymous	
rs4902562	14:68731458	G/A	1.14 (1.09-1.19)	6.15E-10	<i>RAD51B</i> Intronic	
rs2289583	15:75311036	C/A	1.19 (1.14-1.24)	6.22E-15	<i>SCAMP5</i> Intronic	<i>CSK, ULK3, MPI</i>
rs9652601	16:11174365	G/A	1.21 (1.15-1.26)	7.42E-17	<i>CLEC16A</i> Intronic	
rs34572943 (rs9936831)	16:31272353	G/A	1.71 (1.61-1.81)	3.39E-76	<i>ITGAM</i> Intronic	
rs11644034	16:85972612	G/A	1.25 (1.19-1.32)	9.58E-18	16kb 3' of <i>IRF8</i>	
rs2286672	17:4712617	C/T	1.25 (1.16-1.35)	2.93E-09	<i>PLD2</i> Missense	<i>RNF167</i>
rs2941509	17:37921194	C/T	1.35 (1.22-1.49)	7.98E-09	<i>IKZF3</i> 3'-UTR	
rs2304256	19:10475652	C/A	1.24 (1.17-1.31)	3.50E-13	<i>TYK2</i> Missense	
rs7444	22:21976934	T/C	1.27 (1.21-1.33)	1.84E-22	<i>UBE2L3</i> 3'-UTR	<i>UBE2L3</i>

SLE GWAS SNPs taken forward for *cis*-eQTL association analysis. Results from post-replication meta-analysis as described (57). SNP with the lowest P-value post meta-analysis or the SNP with the greatest evidence of a missense effect as defined by a Bayes Factor reported. Autosomal, non-MHC SNPs with MAF > 0.05 included in analysis only (39 total). Risk alleles are highlighted in bold type – minor allele on right. Functional annotation from HaploReg v4.0 using GENCODE genes v10. Stated eGenes detected from microarray studies in LCLs listed as described (57).

Table 2
Details of genotype-expression (eQTL) cohorts used in study

Cohort Name	TwinsUK (MuTHER)			Geuvadis		
Total subjects	856			373		
Ethnicity	EUR (UK)			EUR (CEU, GBR, FIN, TSI)		
Sex	F			M / F		
Age	37–85			NA		
Investigation	Comparison of candidate-causal eQTL and eGene detection between microarray and RNA-Seq			Validation and comparison of LCL RNA-Seq discoveries in whole blood		Identification of asQTLs using RNA-Seq
Citation	<i>Grundberg et. al</i> (9)	<i>Buil et. al</i> (39)	<i>Buil et. al</i> (39)	<i>Buil et. al</i> (39)	<i>Lappalainen et. al</i> (35)	
Expression profile type	Microarray	RNA-Seq	RNA-Seq	RNA-Seq	RNA-Seq	
Unit of expression	Probe	Gene	Meta-exon	Meta-exon	Splice-junction	
Cell-type	LCL	LCL	LCL	Whole Blood	LCL	
Subjects used in analysis	777	683	765	384	373	
Data format	Genevar (summary results)	Read-count	Summary eQTL results	Summary eQTL results	Raw sequence alignments	
RNA Platform	Illumina HT-12 V3	Illumina HiSeq2000		Illumina HiSeq2000	Illumina HiSeq2000	
RNA-Seq mapper	NA	BWA v0.5.9 (GRCh37/hg19)		BWA v0.5.9 (GRCh37/hg19)	GEM v1.349 (GRCh37/hg19)	
Reference transcriptome	NA	GENCODE V10		GENCODE V10	GENCODE V10	
RNA-Seq read length	NA	49-bp PE		49-bp PE	75-bp PE	

Breakdown of genotype-expression (eQTL) cohorts used in analysis. TwinsUK cohort in lymphoblastoid cell lines (LCLs) used for microarray and RNA-Seq comparison (profiled at gene and meta-exon resolution); meta-exons are described as non-redundant overlapping portions of exons generated flattening of the transcriptome annotation. All TwinsUK (MuTHER) samples used in analysis are derived from the original 856 individuals. Validation of LCL data in whole blood carried out at meta-exon level using 384 of the 856 individuals. Geuvadis cohort used for asQTL identification; splice-junction quantifications were generated by Altrans (57) from the raw sequence alignments. Summary eQTL results include only the eQTL association results per test (where full genotype and expression data were not obtainable).

123

Table 3
Candidate-causal eQTLs and associated eGenes detected using microarray (probe-level)

Risk Locus	GWAS SNP	eGene	Probe ID	β	P-Value	FDR (q)
1p13.2	rs2476601	<i>BCL2L15</i>	ILMN_1655722	-0.075	8.26E-04	2.73E-02
3q25.33	rs564799	<i>IL12A</i>	ILMN_1671353	0.113	4.91E-13	4.86E-11
3p14.3	rs11714389	<i>ABHD6</i>	ILMN_1706344	-0.130	1.41E-13	1.63E-11
		<i>PDHB</i>	ILMN_1739274	-0.055	2.55E-05	1.26E-03
4q24	rs10028805	<i>BANK1</i>	ILMN_1661646	0.195	7.98E-13	6.91E-11
8p23.1	rs2736340	<i>BLK</i>	ILMN_1668277	-0.407	7.69E-25	1.07E-22
		<i>FAM167A</i>	ILMN_1687213	0.412	1.48E-43	1.03E-40
15q24.2	rs2289583	<i>CSK</i>	ILMN_1754121	-0.059	9.56E-07	5.10E-05
		<i>MPI</i>	ILMN_1761262	0.058	1.45E-04	5.58E-03
		<i>ULK3</i>	ILMN_1679495	-0.071	1.78E-09	1.12E-07
17p13.2	rs2286672	<i>INCA1</i>	ILMN_1704380	0.035	7.69E-04	2.66E-02
22q11.21	rs7444	<i>UBE2L3</i>	ILMN_1677877	-0.183	4.97E-25	8.61E-23

GWAS SNPs deemed to be candidate-causal eQTLs using microarray expression data profiled from 777 individuals of the TwinsUK cohort in lymphoblastoid cell lines. 768 probes, corresponding to 559 genes, were tested against in cis to the 39 GWAS SNPs.

124

Table 4
Candidate-causal eQTLs and associated eGenes detected using RNA-Seq (Gene-level)

Risk Locus	GWAS SNP	eGene	β	P-Value	FDR (q)
1p13.2	rs2476601	<i>DCLRE1B</i>	-0.330	8.41E-04	1.91E-02
3q25.33	rs564799	<i>IL12A</i>	0.372	1.07E-11	9.70E-10
3p14.3	rs11714389	<i>ABHD6</i>	0.320	7.00E-09	2.28E-07
		<i>RPP14</i>	-0.285	4.15E-07	1.64E-05
4q24	rs10028805	<i>BANK1</i>	-0.316	2.37E-08	1.29E-06
5q31.1	rs17167273	<i>SKP1</i>	-0.564	1.57E-05	5.06E-04
		<i>TCF7</i>	-0.534	2.89E-05	8.27E-04
5q33.3	rs2431697	<i>MIR146A</i>	0.256	1.52E-06	6.89E-05
8p23.1	rs2736340	<i>FAM167A</i>	0.668	1.40E-33	7.62E-31
		<i>BLK</i>	-0.596	3.13E-28	8.51E-26
		<i>RP11-148021.2</i>	-0.591	1.11E-26	2.01E-24
11p15.5	rs2396545	<i>HRAS</i>	-0.248	1.56E-04	4.04E-03
11q13.4	rs3794060	<i>NADSYN1</i>	-0.620	6.43E-24	8.74E-22
		<i>DHCR7</i>	-0.200	1.70E-03	3.43E-02
15q24.2	rs2289583	<i>ULK3</i>	0.303	3.62E-07	1.79E-05
		<i>UBE2Q2</i>	0.249	5.66E-05	1.54E-03
		<i>FAM219B</i>	-0.198	1.18E-03	2.57E-02
		<i>CSK</i>	0.194	1.64E-03	3.43E-02
22q11.21	rs7444	<i>UBE2L3</i>	0.345	2.28E-06	9.54E-05

GWAS SNPs deemed to be candidate causal eQTLs using RNA-Seq expression data profiled from 683 individuals of the TwinsUK cohort in lymphoblastoid cell lines at gene-level resolution. 520 genes were tested against in *cis* to the 39 GWAS SNPs.

125

126

Table 5
Candidate causal eQTLs and associated eGenes detected using RNA-Seq (Exon-level)

Risk Locus	GWAS SNP	eGene	Meta-exon ID (chr. start. end)	β	P-Value	FDR (q)
1p13.2	rs2476601	<i>BCL2L15</i>	1.114420790.114424619	0.226	2.71E-10	1.80E-08
			1.114429871.114430169	0.199	2.72E-08	1.28E-06
			1.114449618.114449783	0.110	2.23E-03	3.85E-02
1q32.1	rs3024505	<i>MAGI3</i>	1.114225519.114228545	0.115	1.41E-03	2.62E-02
			1.207133024.207134568	0.114	1.62E-03	2.94E-02
			1.206945616.206945839	0.174	1.26E-06	4.88E-05
2q24.2	rs2111485	<i>IFIH1</i>	1.207076321.207077484	0.108	2.81E-03	4.63E-02
			2.163123589.163123889	0.119	1.00E-03	1.98E-02
			2.163128736.163128897	0.108	2.69E-03	4.49E-02
			2.163130305.163130454	0.116	1.25E-03	2.37E-02
			2.163136506.163136622	0.138	1.31E-04	3.29E-03
			2.163137838.163138055	0.110	2.34E-03	4.01E-02
			2.163163219.163163680	0.127	4.45E-04	9.72E-03
			3.159996981.159997152	0.109	2.65E-03	4.44E-02
			3.159706537.159706961	0.202	1.66E-08	8.24E-07
			3.159710799.159711631	0.286	7.56E-16	8.33E-14
3q25.33	rs564799	<i>SMC4</i>	3.159713191.159713806	0.281	2.23E-15	2.31E-13
			3.159996981.159997152	0.109	2.65E-03	4.44E-02
			3.160129546.160129872	0.120	8.69E-04	1.74E-02
			3.160137146.160137331	0.112	1.97E-03	3.48E-02
			3.160141213.160141438	0.112	1.98E-03	3.48E-02
			3.160141549.160141628	0.110	2.36E-03	4.03E-02
			3.160149431.160149613	0.126	4.69E-04	1.02E-02
			3.160150071.160150303	0.122	7.51E-04	1.53E-02
			3.160150814.160150997	0.137	1.41E-04	3.47E-03
			3.58223233.58223643	0.132	2.62E-04	6.10E-03
3p14.3	rs11714389	<i>ABHD6</i>	3.58242289.58242432	0.173	1.57E-06	5.89E-05
			3.58252916.58253072	0.174	1.34E-06	5.11E-05
			3.58255048.58255161	0.207	7.18E-09	3.76E-07
			3.58256659.58256791	0.190	1.21E-07	5.27E-06
			3.58260385.58260542	0.200	2.47E-08	1.18E-06
			3.58270924.58271180	0.221	6.02E-10	3.75E-08
			3.58279316.58280461	0.345	7.89E-23	1.13E-20
			4.102946358.102946666	0.264	1.07E-13	9.91E-12
4q24	rs10028805	<i>BANK1</i>	4.102981368.102981546	0.253	1.19E-12	9.92E-11
5q31.1	rs17167273	<i>SKP1</i>	5.133492082.133494319	0.276	7.20E-15	7.17E-13
5q33.3	rs2431697	<i>MIR146A</i>	5.159912306.159914433	0.248	3.36E-12	2.52E-10
			5.159895275.159895447	0.151	2.74E-05	7.97E-04
8p23.1	rs2736340	<i>BLK</i>	8.11351510.11352100	0.462	9.76E-42	3.16E-39
			8.11366659.11367400	0.350	1.72E-23	2.55E-21
			8.11412252.11412398	0.469	5.06E-43	2.01E-40
			8.11414166.11414346	0.448	6.05E-39	1.65E-36
			8.11415471.11415547	0.445	2.13E-38	5.26E-36
			8.11417842.11418961	0.485	2.45E-46	2.11E-43
			8.11420488.11420619	0.440	1.49E-37	2.96E-35
			8.11421412.11422113	0.446	1.32E-38	3.43E-36
			8.11278972.11282145	0.469	3.48E-43	1.64E-40
			8.11301540.11302395	0.463	7.22E-42	2.49E-39
			8.11415975.11416256	0.454	3.63E-40	1.04E-37
			8.11416421.11416495	0.325	2.69E-20	3.67E-18
			8.11417293.11417529	0.395	5.49E-30	9.17E-28
			8.11413760.11414170	0.353	6.24E-24	9.50E-22
			8.11415399.11415531	0.391	2.15E-29	3.48E-27
			11p15.5	rs2396545	<i>ANO9</i>	11.417933.418589
11.418720.419415	0.207	7.70E-09				3.95E-07
11.419582.420860	0.196	4.54E-08				2.06E-06
11.420929.421042	0.163	6.11E-06				2.03E-04
11.428088.428199	0.119	9.93E-04				1.97E-02
11.428475.428639	0.181	4.99E-07				2.07E-05
11.428722.428826	0.164	5.44E-06				1.83E-04
11.429474.430179	0.203	1.52E-08				7.63E-07
11.430269.430403	0.198	3.28E-08				1.52E-06
11.431694.433459	0.144	6.20E-05				1.69E-03
11.433815.433937	0.156	1.45E-05				4.48E-04
11.434024.434098	0.127	4.24E-04				9.30E-03
11.533277.533358	0.136	1.64E-04				3.97E-03
11.533766.533976	0.151	2.72E-05				7.97E-04
11.534212.534375	0.138	1.29E-04				3.24E-03
11.587259.588497	0.126	4.86E-04				1.05E-02
11.597395.597570	0.118	1.03E-03	2.01E-02			
11.607066.609720	0.170	2.37E-06	8.56E-05			
11.611634.612222	0.142	8.00E-05	2.09E-03			
11.561547.561892	0.160	9.26E-06	2.98E-04			

			11.498457.498627	0.152	2.58E-05	7.72E-04
		<i>RNH1</i>	11.504824.505881	0.309	2.28E-18	2.82E-16
			11.507113.507300	0.126	4.55E-04	9.90E-03
		<i>TMEM80</i>	11.700615.701127	0.131	2.75E-04	6.37E-03
			11.71145460.71147019	0.246	5.41E-12	4.00E-10
			11.71148858.71148989	0.172	1.66E-06	6.15E-05
		<i>DHCR7</i>	11.71149795.71150129	0.179	6.25E-07	2.51E-05
			11.71152273.71152486	0.163	5.77E-06	1.93E-04
			11.71153309.71153399	0.207	7.53E-09	3.90E-07
			11.71155003.71155299	0.175	1.14E-06	4.45E-05
			11.71155901.71156004	0.150	3.12E-05	9.03E-04
			11.71175099.71175554	0.227	2.04E-10	1.37E-08
			11.71185441.71186668	0.545	1.79E-60	9.26E-57
			11.71187079.71188484	0.538	1.06E-58	2.75E-55
11q13.4	rs3794060		11.71189441.71190128	0.339	5.32E-22	7.45E-20
		<i>NADSYN1</i>	11.71190340.71191320	0.419	7.54E-34	1.30E-31
			11.71191801.71193071	0.245	6.27E-12	4.57E-10
			11.71195358.71196694	0.280	2.94E-15	2.98E-13
			11.71202880.71202949	0.166	3.68E-06	1.28E-04
			11.71207481.71208657	0.248	3.30E-12	2.51E-10
			11.71209398.71211081	0.196	4.82E-08	2.15E-06
			11.71214910.71216920	0.297	5.05E-17	5.81E-15
		<i>RP11-660L16.2</i>	11.71159720.71159931	0.482	7.76E-46	5.74E-43
			11.71162736.71163203	0.530	1.44E-56	2.49E-53
12q24.12	rs10774625	<i>HECTD4</i>	12.112601913.112602079	0.113	1.81E-03	3.25E-02
			15.75090574.75090653	0.153	2.27E-05	6.82E-04
			15.75091613.75091832	0.140	9.68E-05	2.48E-03
		<i>CSK</i>	15.75092753.75092846	0.143	7.38E-05	1.97E-03
			15.75093164.75093263	0.117	1.15E-03	2.20E-02
			15.75093863.75093936	0.140	1.08E-04	2.76E-03
			15.75094036.75094231	0.167	3.20E-06	1.14E-04
			15.75094338.75094424	0.129	3.65E-04	8.10E-03
		<i>FAM219B</i>	15.75192329.75195127	0.148	4.08E-05	1.15E-03
			15.75182867.75182995	0.150	3.29E-05	9.41E-04
		<i>MPI</i>	15.75185002.75185143	0.250	2.32E-12	1.87E-10
			15.75185479.75185661	0.191	1.08E-07	4.75E-06
15q24.2	rs2289583		15.75189352.75189560	0.212	3.48E-09	1.92E-07
			15.75128459.75129585	0.286	7.98E-16	8.61E-14
			15.75130607.75130685	0.130	3.14E-04	7.11E-03
			15.75130984.75131086	0.142	7.90E-05	2.09E-03
			15.75131351.75131391	0.145	5.99E-05	1.64E-03
		<i>ULK3</i>	15.75131609.75131714	0.182	4.02E-07	1.69E-05
			15.75131899.75132054	0.150	3.16E-05	9.08E-04
			15.75132575.75132657	0.120	8.45E-04	1.70E-02
			15.75132839.75132982	0.133	2.32E-04	5.48E-03
			15.75133746.75133850	0.116	1.35E-03	2.54E-02
			15.75134416.75134536	0.129	3.46E-04	7.79E-03
			15.75134621.75134761	0.130	3.00E-04	6.88E-03
22q11.21	rs7444	<i>UBE2L3</i>	22.21965146.21965332	0.216	1.65E-09	9.46E-08
			22.21975804.21978323	0.422	2.19E-34	4.20E-32

GWAS SNPs deemed to be candidate causal eQTLs using RNA-Seq expression data profiled from 765 individuals of the TwinsUK cohort in lymphoblastoid cell lines at exon-level resolution. 4,786 exons, corresponding to 716 genes were tested against in *cis* to the 39 GWAS SNPs.

128 **RNA-Seq better annotates SLE risk loci by revealing known and novel candidate**
129 **genes**

130 **Fig. 2** illustrates the clear improvement of RNA-Seq relative to microarray in the discovery of
131 candidate-causal eQTLs and their corresponding eGenes when annotating complex-disease
132 susceptibility loci. With RNA-Seq, we replicated known SLE associated eQTLs and eGenes
133 that were previously discovered using microarray. These included rs564799 for *IL12A*,
134 rs2736340 for *BLK*, rs9311676 *ABHD6*, and rs2289583 for *ULK*, *CSK*, and *MPI* (**Tables 4,**
135 **and 5; Table 1** for previously reported associations in LCLs). Several eQTLs for eGenes that
136 have been extensively studied in terms of their role in SLE pathogenesis were consistent
137 across all three platforms: for example, rs10028805 for *BANK1* (57) and rs7444 for *UBE2L3*
138 (58). **Fig. 2** also shows how exon-level RNA-Seq analysis led to the greatest frequency of
139 candidate-causal eQTLs and eGenes than with either gene-level RNA-Seq or microarray (**S1**
140 **Fig.** and **S2 Fig.**). A total of 14 eQTLs modulating expression of 34 eGenes were detected
141 using exon-level RNA-Seq contrasted to 11 eQTLs and 19 eGenes at gene-level RNA-Seq
142 and only 8 eQTLs with 12 eGenes identified using microarray (**S1 Fig.** and **S2 Fig.**). Only
143 one eQTL (rs2286672) and two eGenes (*PDHB*, *INCA1*) were found by microarray
144 exclusively. These associations were either not significant post multiple testing using either
145 RNA-Seq method, or were not deemed candidate-causal (**S1 Table S1** and **S3 Table**). In
146 total 8 eQTLs regulating expression of 27 eGenes were detected using RNA-Seq but missed
147 using microarray (**S3 Fig. S3** and **S4 Fig.**). Interestingly, exon-level analysis led to the
148 greatest frequency of non-candidate-causal associations. Only 14 of the 34 significant
149 eQTLs, $q < 0.05$, showed evidence of a shared causal variant post conditional and
150 colocalisation testing (**S1 Fig.** and **S2 Fig.**).

151

152 Several eGenes known to be involved in the pathogenesis of SLE were identified using
153 RNA-Seq exclusively and not reported in previous microarray-based eQTL studies in LCLs
154 (**Table 1**). These include *IL10*, *IFIH1*, and the microRNA *MIR146A*. We believe a handful of

155 other eGenes unique to RNA-Seq to be novel SLE candidate genes. *NADSYN1* (NAD
156 Synthetase), *HECTD4* (HECT Domain E3 Ubiquitin Protein Ligase 4), *SKP1* (S-Phase
157 Kinase-Associated Protein 1) and *TCF7* (T-cell specific Transcription Factor 7) are examples
158 of novel eGenes.

159

160 RNA-Seq eQTL analysis reveals eQTLs regulating multiple eGenes

161 **Fig. 2** also illustrates that many of the eQTLs discovered using RNA-Seq regulate multiple
162 eGenes. Exon-level analysis generated the greatest ratio (2.42) of candidate-causal eGenes
163 to eQTLs (**S5 Fig.**); suggesting that disease-associated haplotypes may be more functionally
164 potent and harbour multiple gene regulatory effects than previously thought.

165

166 One example of this effect is at the *TCF7-SKP1* locus where the disease-association signal
167 encompasses both genes (**S6 Fig.**). Both *TCF7* and *SKP1* were classified as candidate-
168 causal against the GWAS SNP rs7726414 using gene-level RNA-Seq (**Table 5**), and *SKP1*
169 but not *TCF7* at exon-level (**Table 4**). Interestingly, a missense variant of *TCF7* has been
170 implicated in Type 1 Diabetes risk (59), but there is only weak LD ($r^2 < 0.4$) between this
171 missense variant and rs7726414 (19 kb upstream of *TCF7*) or any protein-coding variants of
172 *TCF7*, suggesting that in SLE the causal mechanism may be dysregulated gene expression
173 of *TCF7* rather than a missense change *per se*. *SKP1*, part of the ubiquitin ligase complex, is
174 thought to stabilize the conformation of E3 ligases and its expression has been shown to be
175 upregulated in lung-cancer (60). Neither of these effects were present in the microarray data
176 as there is another more significant *cis*-eQTL, rs17167273, for the *TCF7* probe
177 (ILMN_1676470), which is not correlated with the rs7726414[T] risk variant ($r^2: 0.02$, **S1**
178 **Table**). In addition, rs7726414[T] was not a significant eQTL for the *SKP1* microarray probe
179 (ILMN_1790710) ($P=0.16$). Our RNA-Seq eQTL analyses indicated that rs7726414[T]
180 represents a novel eQTL for dysregulated gene expression of *SKP1* in SLE (**S6 Fig.**). We

181 believe both *TCF7* and *SKP1* to be highly plausible candidate genes as the literature
182 suggests that knockdown of *TCF7* results in impaired stem cell potency and gene
183 expression regulation of CD34+ cells (61), whilst the mouse knockout of *SKP1* develop
184 highly penetrant T-cell lymphomas (62).

185

186 Other examples where either gene- or exon-level RNA-Seq analysis identified multiple
187 eGenes are at rs3024505 (*IL10*, *IL24*, and *FCAMR*), rs12802200 and rs3794060 (**Fig. 2**). In
188 the immune-gene concentrated 11p15.5 region (**S7 Fig.**), the GWAS SNP rs12802200, is an
189 eQTL for six eGenes, (*HRAS*, *TMEM80*, *RNH1*, *ANO9*, *PHRF1* and *RASSF7*; **Tables 4 and**
190 **5**) following exon- and/or gene-level RNA-Seq analysis, supporting our recent observations
191 of rs12802200 being a *cis*-eQTL for six genes across multiple immune cell-types at this
192 locus (63) and earlier reports demonstrating that rs12802200 was an eQTL for *TMEM80*
193 (whole blood(64)) and for both *RNH1* and *TMEM80* (LCLs (35)). 11p15.5 is also an
194 important regulatory region in non-immune types, because a total of eight eGenes in this
195 region have been identified in multiple non-immune cell types (65), four of which (*HRAS*,
196 *TMEM80*, *RNH1*, *ANO9*) were captured by our RNA-Seq analysis in LCLs. Since SNPs
197 within this susceptibility locus have also been previously shown to be correlated with
198 increased autoantibody production and interferon- α activity in sufferers of SLE (66), further
199 investigation will be required to elucidate a potential mechanism by which dysregulation of
200 gene expression may contribute to these effects. In this gene-dense region (**S7 Fig.**), none
201 of the six candidate-causal eGenes had an annotated microarray probe that passed quality
202 control.

203

204 In the 11q13.4 region, the intronic GWAS SNP rs3794060[C], was classified using gene-
205 level quantification as being a candidate-causal eQTL for both *NADSYN1* (NAD Synthetase
206 1) and *DHCR7* (7-Dehydrocholesterol Reductase) (**Table 4, Fig. 3A and S8 Fig.**). At exon-
207 level resolution, *NADSYN1* was also deemed candidate-causal, as well as the non-coding
208 RNA *RP11-660L16.2* (**Table 5**; described in following section). The risk variant rs3794060[C]

209 has been correlated with reduced circulating 25-hydroxy vitamin D concentrations (67) with
210 reduced vitamin D levels being recently associated with increased disease activity of SLE
211 (68). Interestingly, although a mouse knockout of *DHCR7* showed reduced serum and tissue
212 cholesterol levels (69), no autoimmune phenotype has been described at this locus. Given
213 the role oxidative stress plays in promoting inflammation and triggering autoimmunity
214 through tissue damage (70), it will be interesting to elucidate the role that dysregulation of
215 *NADSYN1* expression plays in this process. Visualization of exon-level association data of
216 *NADSYN1* against rs3794060 suggests a potential splicing mechanism affecting meta-exons
217 11 and 12 ($P=1.79^{E-60}$, 1.06^{E-58} respectively; **Fig. 3B**). The probe for *DHCR7*
218 (ILMN_1815626) showed a weak, but not statistically significant, association with rs3794060
219 ($P=2.9 \times 10^{-03}$), whilst *NADSYN1* had no annotated probe in the microarray dataset.

220

221 **RNA-Seq uncovers the role of non-coding RNA modulation at SLE susceptibility loci**

222 Quantification of non-coding polyadenylated RNAs in the TwinsUK LCL cohort through RNA-
223 Seq revealed three candidate-causal eQTLs influencing the expression of four non-coding
224 eGenes (**Table 6**); none of which were captured using microarray.

225

226 We validated the effect at rs2431697 (5q33.3) where it is documented that the protective
227 minor allele [C] is associated with expression upregulation of the miRNA *MIR146A*, a
228 negative regulator of the type I Interferon pathway (71) (**Fig. 4A**). The best eQTL for
229 *MIR146A* at gene-level was rs2431697 ($P=1.5 \times 10^{-06}$) and also at exon level for both of its
230 exons ($P=3.4 \times 10^{-12}$ and 1.2×10^{-04}). The decrease in rs2431697[T]-dependent expression of
231 *MIR146A* reported in peripheral blood leukocytes of SLE patients disrupts binding of
232 transcription factor Ets-1, uncouples of the type-1 IFN response (71), thereby increasing the
233 inflammatory response.

234

235 **Fig. 4B** shows GWAS variant rs2736340, and other SNPs in tight LD ($r^2 > 0.8$), within the
236 *FAM167A-BLK* (8p23.1) bi-directional promoter region. In this study we detected eQTLs at

237 the known eGenes *BLK* (B lymphocyte kinase) and *FAM167A* (Family with Sequence
238 Similarity 167, Member A) by all quantification methods (**S9 Fig.**). The rs2736340[T] risk
239 allele causes decreased expression of *BLK* ($P=3.2 \times 10^{-28}$) and increased expression of
240 *FAM167A* ($P=1.4 \times 10^{-33}$) at RNA-Seq gene-level (**Table 4**). This effect has been previously
241 described in microarray studies (72) - with reduced promoter activity of *BLK* leading to
242 altered B-cell development (73). The eQTL lies within a region of the genome subject to
243 multiple regulatory effects, with a 24bp region immediately around the variant containing
244 strong chromatin marks (peak height>60) in LCLs for H3K9me3 (gene repression) and
245 H3K4me3 (low expression when present in the promoter of CpG genes) assayed as part of
246 the ENCODE project (**S9 Fig.**). Interestingly, exon-level RNA-Seq analysis revealed that
247 rs2736340 also appeared to modulate the expression of two non-coding RNAs antisense to
248 the 3' region of *BLK*. These are: *RP11-148O21.2* and *RP11-148O21.4* (**Fig. 4B**). The SNP,
249 rs2736340, significantly reduced the expression of both *BLK* and three exons of *RP11-*
250 *148O21.2* and the two exons of *RP11-148O21.4* (**Table 6**). Our analyses indicated that
251 expression disruption of these antisense RNAs caused by SLE risk variants represent a
252 potential novel mechanism at the locus.

253

254 There is an rs3794060 allele-dependent expression modulation of both exons of another
255 non-coding eGene, *RP11-660L16.2I* (**Fig. 4C**), which is located in the bi-directional promoter
256 between *DHCR7* and *NADSYN1*. The best eQTL for those exons is highly correlated with
257 the GWAS SNP (rs2282621, $r^2:0.99$). Both *DHCR7* and *NADSYN1* are candidate-causal
258 eGenes regulated in the same downward direction at RNA-Seq gene-level with respect to
259 the risk allele rs3794060[T] ($P=1.7 \times 10^{-03}$ and $P=6.4 \times 10^{-24}$, respectively) (**S8 Fig. and Table**
260 **4**).

Table 6
Candidate-causal non-coding eGenes discovered using RNA-Seq (exon-level)

Risk Locus	GWAS SNP	eGene	Exon ID (chr. start. end)	β	P-Value	FDR (q)
5q33.3	rs2431697	<i>MIR146A</i>	5.159912306.159914433	0.248	3.36E-12	2.52E-10
			5.159895275.159895447	0.151	2.74E-05	7.97E-04
8p23.1	rs2736340	<i>RP11-148O21.2</i>	8.11415975.11416256	0.454	3.63E-40	1.04E-37
			8.11416421.11416495	0.325	2.69E-20	3.67E-18
		<i>RP11-148O21.4</i>	8.11417293.11417529	0.395	5.49E-30	9.17E-28
			8.11413760.11414170	0.353	6.24E-24	9.50E-22
			8.11415399.11415531	0.391	2.15E-29	3.48E-27
11q13.4	rs3794060	<i>RP11-660L16.2</i>	11.71159720.71159931	0.482	7.76E-46	5.74E-43
			11.71162736.71163203	0.530	1.44E-56	2.49E-53

GWAS SNPs deemed to be candidate causal eQTLs for non-coding eGenes using RNA-Seq expression data profiled from 765 individuals of the TwinsUK cohort in lymphoblastoid cell lines at exon-level resolution.

261

262 **Confirmation of LCL candidate-causal eQTLs and eGenes using whole-blood RNA-**
263 **Seq**

264 To validate our LCL findings in a primary tissue-type, we extended our analytical pipeline to
265 include an exon-level RNA-Seq dataset in 384 whole-blood samples from the TwinsUK
266 cohort (**Table 2**). The full results of these analyses are provided in **S4 Table**.

267

268 We observed good correlation between LCLs and whole-blood effect-sizes (β) of GWAS
269 SNPs against all matched *cis* exon-level associations ($R^2=0.74$; **S10 Fig.**). Seven of the 39
270 GWAS SNPs were classified as candidate-causal eQTLs in whole-blood, modifying 19
271 candidate-causal eGenes (**Table 7**). All seven of the whole-blood eQTLs and 15 of the 19
272 eGenes were deemed candidate-causal in LCLs, suggesting strong conservation across
273 whole-blood cell types (**S11 Fig.**). The remaining four eGenes specific to whole-blood were:
274 *PXK* (rs9311676); *IRF7* and *TALDO1* (rs12802200); and *SCAMP2* (rs2289583) (**Table 7**).
275 Interestingly, the eQTLs regulating these four eGenes in whole-blood also regulated multiple
276 eGenes in LCLs (**S11 Fig.**), implying that they tag highly regulatory haplotypes that may
277 cause cell-type specific gene-expression disruption across the entire locus (same eQTL
278 regulating different eGenes across different cell-types). Three of the four candidate-causal
279 non-coding eGenes from LCLs were found in whole-blood (*RP11-148O21.2*, *RP11-*
280 *148O21.4*, and *RP11-660L16.2*). The LCL-specific *MIR146A* eGene association with GWAS
281 SNP rs2431697 was not deemed to be significant ($P=0.32$), which is likely to be a result of
282 its lymphocyte-specific gene expression profile (71) that is diluted in the heterogeneous
283 population of whole-blood cell-types.

284

285 Inspection of specific exons modulated by the GWAS SNPs in each cell-type revealed
286 instances of variability in the genetic control of exon usage between cell-types. A known
287 splicing event in B-cells caused by branch-point SNP rs17266594 results in the loss of exon
288 2 in susceptibility gene *BANK1* which subsequently leads to B-cell hyper-responsiveness
289 (57) (**S12 Fig.**). In whole-blood the GWAS variant, rs10028805, is associated with altered

290 expression of exon 2 ($P=8.4 \times 10^{-05}$), with the best *cis*-eQTL for this effect being in near-
291 perfect LD (rs4411998; $r^2:0.98$). Both rs10028805 and rs4411998 are in strong LD with the
292 branch-point SNP ($r^2:0.9$). In LCLs however, the best *cis*-eQTL for exon 2, rs4572885
293 ($P=9.74 \times 10^{-23}$), has a large effect but is less correlated with the GWAS SNP ($r^2:0.65$) and
294 conditional analysis judges the effect of the GWAS SNP to be independent to the best *cis*-
295 eQTL for exon 2 (**S3 Table**). Interestingly, there is low correlation between the branch-point
296 SNP rs17266594 and the best *cis*-eQTL for exon 2 in LCLs ($r^2:0.42$); suggesting the
297 regulatory mechanism of exon 2 splicing in *BANK1* may be under two separate genetic
298 influences between the two cell-groups (**S12 Fig.**).

299

300 We saw a near identical pattern of differential exon usage within eGene *NADSYN1* between
301 LCLs and whole-blood driven by the GWAS SNP rs37940460 or tightly correlated variants
302 (**S13 Fig., Table 7**). Variation at rs37940460 appeared to drive extensive expression
303 disruption of two meta-exons (11 and 12) of *NADSYN1* located near the centre of the gene
304 (meta-exon 11: LCL $P=1.79 \times 10^{-60}$; whole-blood $P=1.28 \times 10^{-27}$; meta-exon 12: LCL
305 $P=1.06 \times 10^{-58}$; whole-blood $P=6.30 \times 10^{-26}$). These two meta-exons were deemed to be
306 candidate-causal for SLE across both cell-types. We believe the meta-exons in the 3' end of
307 *NADSYN1* that are candidate-causal in LCLs (**Fig. 3**), are not detected in whole-blood may
308 be because of the smaller sample size or the mixed cell-type composition of the whole blood
309 cohort. This novel instance of specific exon expression disruption found in a primary cell-
310 type at *NADSYN1* may help to resolve the functional consequence of this locus.

311

Table 7
Candidate-causal eQTLs and eGenes detected using RNA-Seq (exon-level) in whole blood

Risk Locus	GWAS SNP	eGene	Exon ID (chr. start. end)	β	P-Value	FDR (q)			
3p14.3	rs9311676	<i>PXK</i>	3.58383332.58383449	0.272	1.15E-07	2.03E-05			
			3.58303167.58305816	0.207	6.18E-05	5.45E-03			
4q24	rs10028805	<i>BANK1</i>	3.58303167.58305920	0.211	4.52E-05	4.07E-03			
			4.102750965.102751363	0.204	8.41E-05	7.11E-03			
			8.11400733.11400856	0.297	6.20E-09	1.40E-06			
			8.11403240.11403612	0.268	1.74E-07	2.94E-05			
			8.11405541.11405634	0.267	2.01E-07	3.26E-05			
			8.11412252.11412398	0.282	3.72E-08	6.86E-06			
			8.11412841.11412993	0.301	3.80E-09	9.63E-07			
			8.11441166.114414346	0.290	1.50E-08	3.04E-06			
			8.11415471.11415547	0.264	2.75E-07	4.29E-05			
			8.11417842.11418961	0.373	1.26E-13	4.65E-11			
8p23.1	rs2736340	<i>BLK</i>	8.11420488.11420619	0.334	4.58E-11	1.33E-08			
			8.11421412.11422113	0.344	1.16E-11	3.62E-09			
			<i>FAM167A</i>	8.11278972.11282145	0.523	2.96E-27	6.00E-24		
			<i>RP11-148O21.2</i>	8.11417293.11417529	0.222	1.79E-05	1.96E-03		
			8.11415975.11416256	0.203	9.13E-05	7.56E-03			
			<i>RP11-148O21.4</i>	8.11413760.11414170	0.220	2.09E-05	2.23E-03		
			<i>ANO9</i>	11.419582.420860	0.180	5.20E-04	3.35E-02		
			<i>HRAS</i>	11.532242.532755	0.179	5.75E-04	3.64E-02		
			11p15.5	rs12802200	<i>IRF7</i>	11.613785.614534	0.263	3.02E-07	4.54E-05
						11.614783.615728	0.216	2.89E-05	2.86E-03
<i>RNH1</i>	11.504824.505881	0.238				3.84E-06	5.02E-04		
<i>TALDO1</i>	11.758950.759057	0.186				3.44E-04	2.36E-02		
<i>NADSYN1</i>	11.71185441.71186668	0.526				1.28E-27	5.19E-24		
11.71187079.71188484	0.512	6.30E-26				8.52E-23			
11q13.4	rs3794060	<i>RP11-660L16.2</i>	11.71159720.71159931	0.437	1.48E-18	8.58E-16			
			11.71162736.71163203	0.508	1.54E-25	1.56E-22			
			<i>CSK</i>	15.75094672.75095539	0.204	8.17E-05	7.05E-03		
15q24.2	rs2289583	<i>MPI</i>	15.75189853.75191798	0.252	1.02E-06	1.43E-04			
			<i>SCAMP2</i>	15.75142855.75143014	0.188	2.83E-04	2.05E-02		
			15.75128459.75129585	0.259	4.62E-07	6.69E-05			
			<i>ULK</i>	15.75132839.75132982	0.189	2.58E-04	1.94E-02		
			15.75134621.75134761	0.194	1.85E-04	1.42E-02			
22q11.21	rs7444	<i>UBE2L3</i>	22.21975804.21978323	0.505	3.68E-25	2.99E-22			

GWAS SNPs deemed to be candidate causal eQTLs using RNA-Seq expression data profiled from 384 individuals of the TwinsUK cohort in whole blood at exon-level resolution. In total, 3,793 exons were tested against, corresponding to 654 genes.

312

313 **Splice-junction quantification reveals asQTLs and additional candidate eGenes**

314 We extended our investigation to determine whether the GWAS SNPs (**Table 1**) had a direct
315 influence on the alternative-splicing of transcripts (alternative-splicing quantitative trait loci;
316 asQTL), and whether expression quantification at this resolution would reveal any additional
317 candidate-genes or potential functional mechanisms. We undertook *cis*-asQTL analysis
318 within a +/-1Mb window around each GWAS SNP against 33,039 splice-junction
319 quantifications, corresponding to 817 genes, in the Geuvadis cohort (**Table 2**). We identified
320 nine asQTLs significantly associated with 62 splice-junctions, corresponding to 10 eGenes
321 (**S5 Table**). After testing for a shared causal variant between the GWAS and asQTL signal,
322 six SLE candidate-causal asQTLs (26 splice-junctions) for seven eGenes remained (**Table**
323 **8**). Four eGenes (*TCF7*, *SKP1*, *BLK*, and *NADSYN1*) had been previously associated
324 through either gene-level or exon-level eQTL mapping using the TwinsUK cohort. The
325 remaining three candidate-causal eGenes detected using asQTL mapping (*IKZF2*, *WDFY4*,
326 and *IRF5*), as well as the novel causal mechanism involving *NADSYN1*, are described
327 below.

328

329 ***IKZF2***

330 *IKZF2* (Ikaros Family Zinc Finger 2) is novel SLE candidate-causal eGene detected only by
331 asQTL analysis. The GWAS association signal around the 3' end of *IKZF2* tagged by risk
332 variant rs3768792[G] drove an increase in the fraction of splicing between exon 6A and exon
333 6B ($P=3.8 \times 10^{-05}$); a bridge that is unique to the truncated isoform (ENST00000413091, 239
334 amino-acids) of *IKZF2* (**Fig. 5A**). Interestingly, this isoform possesses a premature
335 termination codon found on exon 6B that is not found on the canonical isoform
336 (ENST00000457361, 526 amino-acids) as in this isoform, exon 6A is spliced to exon 7 (**Fig.**
337 **5B**). This effect results in the premature truncation of the full-length protein and the
338 subsequent loss of the two zinc-finger dimerization domains found on exon 8 (**Fig. 5B**).
339 *IKZF2* is a transcription factor thought to play a key role in T-reg stabilisation in the presence
340 of inflammatory responses (74). Since the Ikaros transcription factor family primarily regulate

341 gene expression through homo-/hetero-dimerization and DNA binding/protein-protein
342 interactions, the rs3768792[G] dependent asQTL effect on exon 6A to 6B resulting in less
343 functional *IKZF2* could be highly deleterious. *IKZF2* is known to regulate T-reg associated
344 genes, including *IL-2* and *FoxP3* (75, 76), therefore a decrease in the amount of DNA
345 binding *IKZF2* may result in loss of T-reg stability and a decrease of suppressive capacity
346 with consequential autoimmune sequelae. Interestingly, we identified an additional asQTL
347 variant (rs2291241) in near-perfect LD with the rs3768792 GWAS variant ($r^2:0.99$), located 9
348 bp upstream of exon 6B in truncated isoform ENST00000413091 (**S5 Table, Fig. 5C**). This
349 second asQTL, located within the polypyrimidine tract in the exon 6A/exon 6B intron, is a
350 highly plausible driving variant and may act through promotion of the described splicing
351 event (**Fig. 5C**).

352

353 ***WDFY4***

354 We also discovered a novel putative SLE-associated splicing mechanism involving *WDFY4*
355 (*WDFY* Family Member 4), a gene belonging to a family thought to function as master
356 conductors of aggregate clearance by autophagy (77). Risk variant rs2263052[G] or
357 correlated SNPs (**Fig. 6A**) greatly increased the fraction of link-counts between exon 34A
358 and exon 34B ($P=3.3 \times 10^{-19}$) which are unique to the truncated isoform ENST00000374161
359 (**Fig. 6B**). This truncated isoform (552 amino-acids) lacks the two WD40 domains found in
360 the full length isoform (ENST00000325239, 3184 amino-acids) that are essential to
361 enzymatic activity (77). There is a consequential decrease in the fraction of link-counts
362 between exon 34A and exon 35 ($P=3.0 \times 10^{-06}$) that are unique to the canonical isoform of
363 *WDFY4* (**Fig. 6B**). Interestingly, a known missense variant found in exon 31 of *WDFY4* (**Fig.**
364 **6B**), rs7097397 (Arg1816Gln), in strong LD ($r^2:0.7$) with rs2263052, has also been
365 implicated in SLE through GWAS (78). SIFT and PolyPhen predict the amino-acid
366 substitution to be tolerated (0.38) or benign (0.11) respectively (79); thereby suggesting the
367 risk haplotype may harbour two functional mechanisms influencing *WDFY4* (amino-acid
368 change and upregulation of a shorter isoform) that are both involved in SLE pathogenesis.

369

370 ***IRF5***

371 The GWAS SNP and known asQTL, rs3757387, causes differential promoter usage of *IRF5*
372 (Interferon regulatory factor 5); a molecular mechanism that has previously been reported in
373 predisposition of SLE (80). Alteration of a consensus splice-site causes upregulation of a
374 shorter isoform of *IRF5* which subsequently leads to erroneous activation of the type-1 IFN-
375 pathway and pro-inflammatory cytokines (81). We replicated this known effect by observing
376 an increased fraction of splicing of the shorter isoform of *IRF5*, ENST00000489702, with
377 respect to the risk allele rs3757387[C] (**Table 8**). The risk allele increases splicing from the
378 first exon to the penultimate exon of ENST00000489702 ($P=2.2 \times 10^{-08}$); and from the first
379 exon to the final exon of ENST00000489702 ($P=5.9 \times 10^{-07}$).

380

381 ***NADSYN1***

382 Finally, using splice-junction quantification, we were able to pinpoint the specific transcript of
383 *NADSYN1* that drives the exon-level association previously described (**Table 5, Fig. 3**). The
384 GWAS SNP rs3794060 leads to substantial upregulation of the meta-exon 10 to meta-exon
385 12 splice-site ($P=8.0 \times 10^{-12}$) which is unique the ENST00000528509 transcript of *NADSYN1*
386 (**Table 8, S14 Fig.**). As a consequence of this splicing event, it appears the meta-exon 11 to
387 meta-exon 12 splice-site is highly reduced ($P=2.1 \times 10^{-14}$) with reference to the risk allele [C].
388 Meta-exons 11 and 12 were implicated in exon-level analysis but a specific transcript could
389 not be isolated as the gene annotation was not collapsed to the granularity used in the
390 asQTL analysis. Interestingly, transcript ENST00000528509 is translated to a 294 amino
391 acid residue protein where the canonical transcript of *NADSYN1*, ENST00000319023, is 706
392 amino acids. The shorter protein lacks the NAD(+) Synthetase domain (located in positions
393 339-602aa) found in the canonical protein (Pfam: PF02540); thus implicating loss of this
394 domain as a potential causal mechanism.

395

Table 8
Candidate-causal asQTLs and associated eGenes detected using RNA-Seq (Splice-junction level)

Risk Locus	GWAS SNP	eGene	Splice Junction (chr: donor-acceptor exon)	β	P-Value	FDR (q)
2q34	rs3768792	IKZF2	2:213872084.213872808-213886368.213886444	-0.04	3.64E-09	5.51E-06
			2:213878515.213880002-213886368.213886444	-0.03	1.30E-06	1.07E-03
			2:213881647.213881768-213886368.213886444	-0.04	1.48E-07	1.41E-04
			2:213886717.213886854-213886368.213886444	0.07	3.80E-05	1.93E-02
			2:213914437.213914604-213886368.213886444	-0.04	4.55E-06	3.15E-03
5q31.1	rs7726414	SKP1	5:133541305.133541822-133561451.133561762	0.02	1.42E-06	1.16E-03
			5:133541645.133541822-133561451.133561762	-0.03	1.28E-06	1.07E-03
7q32.1	rs3757387	TCF7	5:133478412.133478791-133474642.133474729	0.01	1.90E-06	1.49E-03
			7:128585899.128586088-128577666.128577888	0.02	2.18E-08	2.49E-05
8p23.1	rs2736340	BLK	7:128586555.128586616-128577666.128577888	0.05	9.51E-07	8.13E-04
			8:11351510.11352100-11403561.11403612	0.10	4.16E-05	2.08E-02
			8:11400733.11400856-11403561.11403612	-0.04	6.24E-05	2.96E-02
			8:11407668.11407771-11403240.11403612	0.02	1.74E-09	3.14E-06
			8:11412252.11412398-11403240.11403612	0.02	2.77E-09	4.61E-06
			8:11414167.11414297-11407503.11407771	0.01	1.36E-08	1.64E-05
			8:11415471.11415547-11407503.11407771	0.01	2.52E-06	1.90E-03
			8:11415471.11415547-11414166.11414346	-0.04	3.24E-06	2.32E-03
			8:11420488.11420619-11414166.11414346	0.02	1.09E-13	7.06E-10
			10:50031227.50032214-50030425.50030582	-0.02	3.31E-19	2.15E-14
10q11.23	rs2663052	WDFY4	10:50034716.50034954-50030425.50030582	0.02	3.01E-06	2.17E-03
			11:71171087.71171259-71171768.71171993	-0.06	2.95E-05	1.55E-02
11q13.4	rs3794060	NADSYN1	11:71184324.71184412-71187247.71188271	0.17	8.00E-12	2.08E-08
			11:71184615.71184732-71187079.71188484	0.06	1.02E-04	4.51E-02
			11:71185441.71186668-71187247.71188271	-0.19	2.13E-14	1.73E-10
			11:71185441.71185572-71189441.71189515	0.02	1.06E-05	6.71E-03
			11:71185441.71186668-71187079.71188484	-0.06	1.02E-04	4.51E-02

GWAS SNPs deemed to be candidate causal asQTLs using RNA-Seq expression data profiled from 373 individuals of the Geuvadis cohort in lymphoblastoid cell lines at splice-junction resolution. 33,039 splice-junctions, corresponding to 817 genes were tested against in cis to the 39 GWAS SNPs.

396

397 Discussion

398 Detailed characterization of the functional effects of human regulatory genetic variation
399 associated with complex-disease is paramount to our understanding of molecular aetiology
400 and poised to make significant contributions to translational medicine (82). Use of eQTL
401 mapping studies to interpret GWAS findings have proved fundamental in our progression
402 towards this goal - through prioritization of candidate genes, refinement of causal variants,
403 and illumination of mechanistic relationships between disease-associated genetic variants
404 and gene expression (82, 83). However, there is often a disparity between disease-
405 associated genetic variation and phenotypic alteration, which historically may be due to the
406 use of microarray-based technologies to profile genome-wide gene expression. With the
407 advent of RNA-Seq, we can achieve more accurate quantification of the mRNA output of
408 genes, individual exons, and isoform abundance, as well as unannotated and non-coding
409 transcripts. Detection of splicing variants at susceptibility loci using RNA-Seq has the
410 potential to uncover the role of specific isoforms implicated in disease risk, which are likely to
411 have remained concealed by microarray, as a largely independent subset of variants control
412 alternative splicing of isoforms compared to overall gene abundance (35).

413

414 Our two major motivations for this study were firstly to directly compare the ability of RNA-
415 Seq with microarrays to detect candidate-causal eQTLs and their associated eGenes from
416 GWAS data, and then to assess each platform's effectiveness in explaining the potential
417 causal genes and mechanisms implicated by SLE risk alleles. A previous investigation of the
418 same SLE risk alleles used in this study with eQTL data from LCL microarray datasets
419 revealed that only 13 of the 39 risk alleles were eQTLs for a total of 15 eGenes (**Table S6**).
420 Therefore, in an attempt to increase our understanding of the extent to which eQTLs can
421 explain the functional consequences of our risk alleles and to achieve both of our major aims
422 for this investigation, we set up an analytical pipeline to compare the results of eQTL
423 annotation for 39 SLE susceptibility loci with *cis*-eQTL data from both microarray and RNA-

424 Seq experiments from the TwinsUK cohort in LCLs. We incorporated steps to minimize
425 false-positive associations through conditional and colocalisation analysis, as approximately
426 34% of all genes have a second independently associated *cis*-eQTL for any of their exons
427 when conditioning on the best *cis*-eQTL (35). The analytical pipeline we present will be
428 applicable to the functional annotation of susceptibility loci from a wide range of human
429 diseases.

430

431 **Fig. 7** summarises the data generated in this manuscript illustrating which of the GWAS
432 SNPs show evidence of a candidate-causal eQTL association across the quantification
433 types. Our data analysis revealed that RNA-Seq is a more powerful in the identification of
434 candidate-causal eQTLs and their accompanying eGenes than corresponding microarray
435 datasets (**S6 Table**). Many of the published SLE candidate eGenes and associated
436 mechanisms were well-replicated by performing *cis*-eQTL analysis of RNA-Seq datasets at
437 various resolutions for each of the GWAS variants. These eGenes included, among others,
438 the effect of risk variants at *BLK* and *FAM167A* (**S9 Fig.**), *MIR146A* (**Fig. 4A**), *BANK1* (**S12**
439 **Fig.**) and *IRF5*. Microarray studies were unable to detect the novel SLE candidate-causal
440 eGenes identified from RNA-Seq data including *NADSYN1*, *TCF7*, *SKP1*, *WDFY4*, *IKZF2*,
441 and the non-coding RNA genes: *RP11-148O21.2*, *RP11-148O21.4*, and *RP11-660L16.2*
442 (**Fig. 2**).

443

444 Our results also demonstrate that RNA-Seq analysis is much better than microarrays in
445 identifying multiple eGenes for a single SNP (that may tag multiple functional variants). An
446 increased ratio of eQTLs to eGenes (average number of eGenes per candidate-causal
447 eQTL) was observed using RNA-Seq at exon-level (2.42) compared with gene-level (1.72)
448 and which were both greater than microarray (1.5) (**S5 Fig.**). The ability of RNA-Seq exon-
449 level analysis to identify multiple target eGenes for a specific eQTL is supported by recent
450 observations from capture Hi-C (cHi-C) experiments to functionally annotate chromatin
451 interactions, such as enhancer–promoter interfaces (84, 85). It has been shown that

452 chromatin interactions can control transcription in both *cis* and *trans* in a largely sequence-
453 specific manner, thus it is likely that some GWAS variants may functionally act through the
454 disruption of chromatin dynamics resulting in perturbation of expression of multiple genes
455 (84, 86, 87). Specific instances of this type of effect are seen in colorectal cancer risk loci
456 where the risk locus 11q23 mapped to interactions with genes *C11orf53*, *C11orf92* and
457 *C11orf93*, and separately, the risk SNP rs6983267 within 8q24 disrupts a chromatin
458 regulatory network involving interactions between three genes *CCAT2*, *CCAT1* and *MYC*
459 (84). Our results support this notion of multiple perturbed genes at a single susceptibility
460 locus. At 1q32.1, for example, rs3024505 was found to be associated with three plausible
461 candidate-causal eGenes: *IL10*, *IL24*, and *FCAMR* (located 1 kb, 130 kb, and 191 kb away
462 from rs3024505 respectively). These chromatin capture data also support the argument of
463 using RNA-Seq and extending the *cis*-eQTL distance (typically +/-0.25–1Mb) to a larger
464 region (+/-5Mb) around the associated SNP to identify effects caused by chromatin
465 interactions over a larger distance than commonly designated as *trans* from eQTL-type
466 analyses (88). Integration of eQTL data with epigenetic regulation (promoter methylation,
467 histone modification and expression of non-coding RNA) will allow the identification of the
468 potential mechanism of action (disruption of epigenetic landscape) and disease biology of
469 associated variants.

470

471 We have also demonstrated the power of RNA-Seq compared with microarray in the
472 discovery of alternative-splicing events. This is of significant importance as approximately
473 80% of all human genes undergo alternative splicing and it is estimated that 20-30% of
474 disease-associated mutations modify the configuration of expressed isoforms (89, 90). A
475 recent study has concluded that regulatory variants controlling gene splicing are major
476 contributors to complex traits (91). Two examples of this taken from our analyses are the risk
477 alleles at the *IKZF2* and *WDFY4* loci which drive up-regulation of short isoforms. Neither of
478 these effects were captured by the microarray probes that targeted the 3'-UTR of the
479 canonical longer isoforms. At *WDFY4*, the splicing variant rs2263052[G] is in strong LD with

480 an (Arg1816Gln) missense variant rs7097397[G], which we showed to be associated with
481 SLE (**Fig. 6**). These two potentially causal signals may reinforce each other. The novel
482 association identified in our group's recent GWAS study (63) at the *IKZF2* locus implicated a
483 risk haplotype tagged by the risk allele of rs3768792[G]. We identified, by RNA-Seq splice-
484 junction quantification exclusively, that variation at the rs3768792[G] risk allele led to
485 increased production of a shorter isoform of *IKZF2* (**Fig. 5**). Interestingly, other members of
486 this gene family, *IKZF1* and *IKZF3*, are also associated with SLE (63). An associated variant
487 in the 3'-UTR of *IKZF1* has been associated with increased expression of genes of the type
488 1 IFN pathway and decreased expression of complement genes, both mediated in *trans*
489 (64). The functional effect of the *IKZF3* common variant is less well documented, although
490 *IKZF3* knockout mice develop spontaneous autoantibodies and B-cell lymphoma (92). The
491 *IKZF2* knockout mouse has not been characterised for immune-deficient phenotypes. We
492 hypothesize that upregulation of the shorter isoform of *IKZF2* caused by rs3768792[G],
493 which lacks the dimerization domain, reduces translocation of the protein into the nucleus
494 and regulation of transcription of target genes. We believe this aberrant mechanism may
495 result in loss of T-reg stability. The asQTL discoveries described in this manuscript are
496 examples of how RNA-Seq can suggest a potential causal mechanism that can be easily
497 validated experimentally.

498

499 Our study also demonstrates that RNA-Seq is able to identify disease-relevant non-coding
500 RNAs. These type of transcripts have long been known to be of relevance to human
501 disease, however their detection and functional importance may have been under-estimated.
502 We identified three novel non-coding anti-sense RNAs using RNA-Seq: two regulated by
503 rs2736340 (*RP11-148O21.2* and *RP11-148O21.4*) (**Fig. 4B**), and one regulated by
504 rs3794060 (*RP11-660L16.2*) (**Fig. 4C**). These findings were replicated in whole blood (**Table**
505 **7**).

506

507 The data we present in this manuscript demonstrate that a comprehensive integrated
508 approach for eQTL analysis should be undertaken at gene-, exon- and exon-junction level
509 quantification. Excluding one or more levels of analysis will mean that eQTLs and/or eGenes
510 may be missed. This is illustrated by a number of examples in **Fig. 7**. At some loci, there
511 was an exon-level effect, which was not observed at the gene-level. For example, the risk
512 allele rs3024505[A] was an eQTL for *IL10*, *IL24*, and *FCAMR* at exon-level resolution only
513 (**Table 5**), but none of these eGenes were deemed to be significant at gene-level. This
514 suggests that the exon-level effect is more targeted than gene-level quantification, where
515 multiple different effects across the gene may dilute out the signal. However, some eGenes
516 exhibit a probable whole gene-level effect (*UBE2L3*, *BLK*, and *FAM167A*) as every
517 expressed exon showed a candidate-causal association for the respective risk alleles.
518 Hierarchical clustering tests could be designed to distinguish between these genuine gene-
519 level and exon-level effects, such as at *NADSYN1* or *BANK1*, where the gene-level effect is
520 likely to be driven by only a subset of exons (**Fig. 3**, **S12 Fig.**). There were occurrences
521 where significant candidate-causal eGenes were detected but there was no effect at the
522 exon-level. At *TCF7*, variants in low LD with rs7726414 exhibited significant exon-level *cis*-
523 eQTLs (**S3 Table**) and were deemed to be independent of the disease-association.
524 However, gene-level analysis revealed that the risk rs7726414 variant was candidate-causal
525 for total *TCF7* expression (**S2 Table**). These results emphasise that for any given eGene
526 there may be multiple genetic effects at different resolutions of quantification.

527

528 We understand the limitation of LCLs for transcript profiling studies. There is an inherent
529 limitation analysing LCL expression datasets, such as those available for our study, because
530 although LCLs are a good surrogate model for primary B-cells, the effect of EBV
531 transformation is likely to disrupt their underlying epigenetic and transcriptomic background.
532 The percentage of asQTLs in LCLs will exhibit significantly less replication in primary cell
533 types because of cell-type variability in the genetic control of isoform usage, approximately
534 70% of *cis*-eQTL detected in LCLs can be replicated in a primary tissue type (33). The

535 significance of alternative-splicing in genomic medicine will become better understood once
536 large RNA-Seq based eQTL cohorts emerge across a multitude of disease-relevant cell-
537 types. A gold standard of candidate-causal eQTL mapping strategies using RNA-Seq across
538 datasets using an explicit set of quantification types (gene-, exon-, splice-junction, isoform)
539 and analytical pipelines, will accelerate this process.

540

541 In summary, we have demonstrated the effectiveness of eQTL analysis using RNA-Seq by
542 increasing the numbers of candidate eGenes regulated by SLE associated alleles (**Fig. 2**,
543 **Fig. 7**, and **S6 Table**). We have shown that the power of RNA-Seq in eQTL annotation of
544 GWAS loci lies not only the assessment of the variants regulating the expression of
545 candidate genes, but also in uncovering putative molecular mechanisms, which allow for
546 more refined targeted follow-up studies to assess the phenotypic consequence of the
547 disease-associated variant. These studies could include knocking down target gene or
548 introducing recombinant vectors *in vitro* to overexpress target genes to evaluate phenotypic
549 consequence of expression changes of specific loci. Site directed mutagenesis could be
550 used to introduce candidate causal splice-sites and over-express target isoforms. The
551 CRISPR/Cas9 system for targeted genome editing presents an exciting opportunity for
552 eQTL/RNA-Seq targeted follow-up studies and the investigation of the effect that specific
553 variants have on the expression profile across different cell types.

554 **Materials and Methods**

555 **Selection of SLE associated SNPs**

556 SLE associated SNPs were taken from our recent 2015 publication (63). The study
557 comprised a primary GWAS, with validation through meta-analysis and replication study in
558 an external cohort (7,219 cases, 15,991 controls in total). The independently-associated
559 susceptibility loci taken forward for this investigation were those that passed either genome-
560 wide significance ($P < 5 \times 10^{-08}$) in the primary GWAS or meta-analysis and/or those that
561 reached significance in the replication study (False Discovery Rate, $q < 0.01$). We
562 defined the 'GWAS SNP' at each locus as either being the SNP with the lowest P -value post
563 meta-analysis or the SNP with the greatest evidence of a missense effect as defined by a
564 Bayes Factor. We omitted non-autosomal associations and those within the Major
565 Histocompatibility Complex (MHC), and SNPs with a MAF < 0.05 . In total, 39 GWAS SNPs
566 were taken forward (**Table 1**).

567

568 **TwinsUK cohort eQTL datasets**

569 Expression profiling by microarray (9) and RNA-Seq (39) of individuals from the UK Adult
570 Twin Registry (TwinsUK) was carried out in two separate studies on the MuTHER (Multiple
571 Tissue Human Expression Resource) cohort (**Table 2**). The MuTHER cohort is composed of
572 856 healthy female individuals of European descent aged between 37-85 years. We
573 considered expression quantification data from both resting LCLs and whole blood. Profiling
574 by microarray was performed using the Illumina Human HT-12 V3 BeadChips. For RNA-
575 Seq, samples were sequenced using the Illumina HiSeq2000 and the 49-bp paired-end
576 reads mapped with BWA v0.5.9 to the GRCh37 reference genome. Exons ('meta-exons'
577 created by merging all overlapping exonic portions of a gene into non-redundant units) were
578 quantified using read-counts against the GENCODE v10 annotation; with gene quantification
579 defined as the sum of all exon quantifications belonging to the same gene. Full quality
580 control and normalization procedures are described in the respective articles. Data from

581 each of the TwinsUK eQTL studies (**Table 2**) were provided in different formats. In each
582 instance it was necessary to generate summary *cis*-eQTL statistics per GWAS SNP (SNP,
583 expression-unit, β , standard error of β , and *P*-value of association) for integration analysis.
584 Per quantification type (microarray, RNA-Seq gene-level, and exon-level), each GWAS SNP
585 was subject to *cis*-eQTL analysis against all expression-units within +/-1Mb using no *P*-value
586 threshold. If the GWAS SNP was not found in an eQTL dataset, the most highly correlated,
587 closest tag SNP with $r^2 \geq 0.7$, common to all datasets, was used as its proxy (**Table 1**).
588 Adjustment for multiple testing of *cis*-eQTL results per quantification type were undertaken
589 using FDR with $q < 0.05$ deemed significant.

590

591 *Microarray cis-eQTL mapping*

592 We used the Genevar (GENe Expression VARiation) portal to generate summary-level *cis*-
593 eQTL results (50). We ran the association between normalized expression data of the 777
594 individuals and each GWAS SNP implementing the external algorithm option (two-step
595 mixed model-based score test). In total 768 probes (559) genes, were tested.

596

597 *RNA-Seq (gene-level) cis-eQTL mapping*

598 RNA-Seq gene-level quantification was provided as residualized read-counts (effect of family
599 structure and other covariates regressed out). We had full genetic data for 683 individuals
600 and performed the analysis of each GWAS SNP against the transformed residuals using the
601 linear-model function within the MatrxieQTL R package (93). 520 genes were tested against
602 in *cis*.

603

604 *RNA-Seq (exon-level) cis-eQTL mapping*

605 *P*-values from the association of all SNPs against exon-level quantifications for 765
606 individuals using linear-regression were provided. We generated the t-statistic using the
607 lower-tail quantile function t-distribution function in R with 763 degrees of freedom. The

608 standard error and β were derived from the t-statistic. We then extracted the summary *cis*-
609 eQTL results for each GWAS SNP. 4,786 exons, corresponding to 716 genes for testing.

610

611 **SLE candidate-causal *cis*-eQTL classification**

612 *Conditional analysis*

613 We used the COJO (conditional and joint genome-wide association analysis) function of the
614 GCTA (Genome-wide Complex Trait Analysis) application to determine whether the GWAS
615 SNP had an independent effect on expression from that of the best *cis*-eQTL (55). For each
616 significant association ($q < 0.05$), we re-performed the analysis using all SNPs within +/-1Mb
617 of the expression-unit in hand. We used the available genotype information of the 683
618 TwinsUK individuals to extract allele coding along with the MAF, and integrated this with the
619 *cis*-eQTL summary data. We discarded SNPs with: MAF < 0.05, imputation call-rates < 0.8,
620 and HWE $P < 1 \times 10^{-4}$. We used these individuals as the reference panel to calculate local
621 pairwise linkage disequilibrium (LD) between variants. Per significant association, all *cis*-
622 eQTLs were conditioned on by the best *cis*-eQTL. We then extracted the conditional *P*-value
623 of the GWAS SNP and considered associations to be independent to the best *cis*-eQTL if
624 $P_{\text{cond}} < 0.05$.

625

626 *Colocalisation Analysis*

627 We employed the 'coloc' Bayesian statistical method using summary data implemented in R
628 to test for colocalisation between *cis*-eQTL and disease causal variants derived from the
629 GWAS (56). The method makes the assumption of there being a single causal variant for
630 each trait (disease association and gene-expression from two separate studies) per locus
631 and calculates the posterior probabilities under five different causal variant hypotheses:
632 association with neither trait (H0), association with one trait but not the other (H1, H2),
633 association with both traits but from independent signals, and association with both traits
634 with a shared causal signal (H4). We extracted the necessary SNP statistics for the disease-
635 associated regions from our own GWAS and applied the same SNP filters used in the

636 conditional analysis. We tested for colocalisation between the GWAS summary data and *cis*-
637 eQTL data for each significant association within a +/-1Mb window of the GWAS SNP. We
638 assigned the prior probabilities, p_1 and p_2 (SNP is associated with GWAS and gene
639 expression respectively), as 1×10^{-04} i.e. 1 in 10,000 SNPs are causal to either trait, with p_{12}
640 (SNP is associated with both traits) as 1×10^{-06} or 1 in 100 SNPs associated with one trait are
641 also associated with the other. For each *cis*-eQTL association colocalisation test, if the
642 posterior probability PP3 (two distinct causal variants, one for each trait) is greater than PP4
643 (single causal variant common to both traits), then greater posterior support is given to the
644 hypothesis that independent causal variants exist in both traits and thus the eQTL is unlikely
645 to be attributed to SLE genetic association.

646

647 **Definition of SLE candidate-causal *cis*-eQTL and eGene**

648 We defined a GWAS SNP as an SLE candidate-causal *cis*-eQTL if it met the following
649 criteria: significant post-multiple testing adjustment ($q < 0.05$), not independent to the best
650 *cis*-eQTL from conditional analysis ($P_{\text{cond}} > 0.05$), and supporting evidence of a shared
651 causal variant between gene expression and the primary GWAS signal based on
652 colocalisation ($PP3 < PP4$). The gene whose expression is modulated by the candidate-
653 causal eQTL is defined as an SLE candidate-causal eGene (**Fig. 1**).

654

655 **Validation of LCL SLE candidate-causal *cis*-eQTLs in whole blood**

656 *Cis*-eQTL summary data from whole blood at RNA-Seq exon-level were made available for
657 384 individuals of the 856 TwinsUK cohort individuals (**Table 2**). Expression profiling and
658 genotyping were identical to that as described for LCLs. We applied the same methodology
659 to this dataset to generate full *cis*-eQTL summary statistics, perform conditional and
660 colocalisation analysis, and classify SLE candidate-causal eQTLs and associated eGenes
661 (**Fig. 1**). In total, 3,793 exons were tested against, corresponding to 654 genes.

662

663 **Geuvaris SLE candidate-causal *cis*-eQTL analysis**

664 We investigated SLE disease-associated alternative splicing QTLs (asQTLs) using
665 European samples from the raw alignment files of the Geuvadis (35) 1000 Genomes RNA-
666 Seq project profiled in LCLs (**Table 2**). Genotype data and read-alignments were
667 downloaded from ArrayExpress for the 373 Europeans (comprising 91 CEU, 95 FIN, 94
668 GBR, and 93 TSI). We performed PCA on chromosome 20 using the R/Bioconductor
669 package SNPRelate (94) and decided to include the first three principle components as
670 covariates in the eQTL model as well as the binary imputation status (mixture of Phase 1
671 and Phase 2 imputed individuals). We removed SNPs with $MAF < 0.05$, imputation call-
672 rates < 0.8 , and HWE $P < 1 \times 10^{-04}$. We removed non-uniquely mapped, non-properly paired
673 reads, and reads with more than eight mismatches for read and mate using Samtools(95).
674 We used the Altrans (96) method against GENCODE v10 to generate relative quantifications
675 (link-counts) of splicing events; which in brief, utilizes split and paired-end reads to count
676 links between exon-boundaries, which themselves are created by flattening the annotation
677 into unique non-redundant exon-groups. Following PCA of the link-counts, we decided to
678 normalize all link-counts with the first 10 principle components then removed exon-
679 boundaries with zero links in more than 10% of individuals. Link-counts were converted to
680 link-fractions (coverage of the link over the sum of the coverage of all the links that the first
681 exon makes) and merged in both 5'-3' and 3'-5' directions. Per GWAS SNP we performed
682 *cis*-eQTL analysis against the normalized link-fractions in MatrixeQTL with a linear-model
683 (93). 33,039 link-fractions were tested against corresponding to 817 genes in total. After
684 FDR multiple-testing adjustment we considered associations with $q < 0.05$ as significant. As
685 full genetic and expression data were available, we decided to use the Regulatory Trait
686 Concordance (RTC) method to assess the likelihood of a shared functional variant between
687 the GWAS SNP and the asQTL signal (48). For each significant asQTL association we
688 extracted the residuals of the linear-regression of the best *cis*-eQTL against normalized link-
689 fractions and re-performed the analysis using all SNPs within the defined hotspot interval
690 against this pseudo-phenotype. The RTC score was defined as $(N_{SNPs} - Rank_{GWAS\ SNP}) / N_{SNPs}$
691 where N_{SNPs} is the number of SNPs in the interval, and $Rank_{GWAS\ SNP}$ is the rank of the

692 GWAS SNP association P -value against all other SNPs in the interval. We classified an SLE
693 candidate-causal *cis*-asQTL as a GWAS SNP with a significant association ($q < 0.05$) with
694 link-fraction quantification and an RTC score > 0.9 .

695

696 **Statistical analysis and data visualisation**

697 We performed statistical analysis, graphics and data handling in R version 3.2.0 and ggplot2.

698 Genetic plots were generated using LocusZoom v1.1 (97). Karyotype diagrams were

699 modified from Ensembl (98). GWAS association plots and gene annotation graphic

700 visualisations were created using the UCSC Genome Browser(99).

701 **Acknowledgements**

702 DSCG and TJV were awarded an Arthritis Research UK PhD Studentship (for CO) (20332)
703 “SLE pathogenesis: the molecular basis for multiple association signals in *IKZF2*” to
704 undertake the analyses described in this manuscript. DSCG, DLM and TJV were awarded
705 an Arthritis Research UK Project Grant (20265) “Post GWAS: A Functional Genomic
706 Analysis of the SLE Susceptibility Gene *IKZF1*”, which supported AC. TJV received funds
707 from China Scholarship Council, number 201406380127 for LC. ALR was supported by
708 MRC project grant L002604/1 “Functional Genomics of SLE: A Trans-ancestral approach”
709 and an ARUK project grant (20580) “Targeted DNA sequencing in Indian and European
710 samples contributes to causal allele identification for lupus”. KSS was awarded funding by
711 the MRC (MR/L01999X/1 and MR/M004422/1).

712 The Geuvadis 1000 Genomes RNA-Seq data was downloaded from the EBI ArrayExpress
713 Portal (accessions E-GEUV-1). The RNA-Seq data on the TwinsUK samples in both LCLs
714 and whole blood was made available through the EUROBATS project (EGAS00001000805
715 from the European Genome-Phenome Archive). The expression microarray data on the
716 TwinsUK samples was downloaded from the EBI ArrayExpress Portal (E-TABM_1140).

717 The TwinsUK study was funded by the Wellcome Trust; European Community's Seventh
718 Framework Programme (FP7/2007-2013). The study also receives support from the National
719 Institute for Health Research (NIHR)- funded BioResource, Clinical Research Facility and
720 Biomedical Research Centre based at Guy's and St Thomas' NHS Foundation Trust in
721 partnership with King's College London. SNP Genotyping was performed by The Wellcome
722 Trust Sanger Institute and National Eye Institute via NIH/CIDR.

723 **Conflict of Interest Statement**

724 The authors declare that there are no conflicts of interest.

725

726 **References**

- 727 1. Hindorff,L.A., Sethupathy,P., Junkins,H.A., Ramos,E.M., Mehta,J.P., Collins,F.S. and
728 Manolio,T.A. (2009) Potential etiologic and functional implications of genome-wide
729 association loci for human diseases and traits. *Proc. Natl. Acad. Sci. U. S. A.*, **106**,
730 9362–7.
- 731 2. Maurano,M.T., Humbert,R., Rynes,E., Thurman,R.E., Haugen,E., Wang,H.,
732 Reynolds,A.P., Sandstrom,R., Qu,H., Brody,J., *et al.* (2012) Systematic Localization of
733 Common Disease-Associated Variation in Regulatory DNA. *Science (80-.)*, **337**,
734 1190–1195.
- 735 3. The ENCODE Project Consortium, Dunham,I., Kundaje,A., Aldred,S.F., Collins,P.J.,
736 Davis,C. a, Doyle,F., Epstein,C.B., Fietze,S., Harrow,J., *et al.* (2012) An integrated
737 encyclopedia of DNA elements in the human genome. *Nature*, **489**, 57–74.
- 738 4. Kundaje,A., Meuleman,W., Ernst,J., Bilenky,M., Yen,A., Heravi-Moussavi,A.,
739 Kheradpour,P., Zhang,Z., Wang,J., Ziller,M.J., *et al.* (2015) Integrative analysis of 111
740 reference human epigenomes. *Nature*, **518**, 317–330.
- 741 5. Forrest,A.R.R., Kawaji,H., Rehli,M., Kenneth Baillie,J., de Hoon,M.J.L., Haberle,V.,
742 Lassmann,T., Kulakovskiy,I. V., Lizio,M., Itoh,M., *et al.* (2014) A promoter-level
743 mammalian expression atlas. *Nature*, **507**, 462–470.
- 744 6. Nicolae,D.L., Gamazon,E., Zhang,W., Duan,S., Dolan,M.E. and Cox,N.J. (2010) Trait-
745 associated SNPs are more likely to be eQTLs: annotation to enhance discovery from
746 GWAS. *PLoS Genet.*, **6**, e1000888.
- 747 7. Stranger,B.E., Montgomery,S.B., Dimas,A.S., Parts,L., Stegle,O., Ingle,C.E.,
748 Sekowska,M., Smith,G.D., Evans,D., Gutierrez-Arcelus,M., *et al.* (2012) Patterns of cis
749 regulatory variation in diverse human populations. *PLoS Genet.*, **8**, e1002639.
- 750 8. Spielman,R.S., Bastone,L.A., Burdick,J.T., Morley,M., Ewens,W.J. and Cheung,V.G.

- 751 (2007) Common genetic variants account for differences in gene expression among
752 ethnic groups. *Nat. Genet.*, **39**, 226–231.
- 753 9. Grundberg,E., Small,K.S., Hedman,Å.K., Nica,A.C., Buil,A., Keildson,S., Bell,J.T.,
754 Yang,T.-P., Meduri,E., Barrett,A., *et al.* (2012) Mapping cis- and trans-regulatory effects
755 across multiple tissues in twins. *Nat. Genet.*, **44**, 1084–1089.
- 756 10. Fairfax,B.P., Makino,S., Radhakrishnan,J., Plant,K., Leslie,S., Dilthey,A., Ellis,P.,
757 Langford,C., Vannberg,F.O. and Knight,J.C. (2012) Genetics of gene expression in
758 primary immune cells identifies cell type–specific master regulators and roles of HLA
759 alleles. *Nat. Genet.*, **44**, 502–510.
- 760 11. Naranbhai,V., Fairfax,B.P., Makino,S., Humburg,P., Wong,D., Ng,E., Hill,A.V.S. and
761 Knight,J.C. (2015) Genomic modulators of gene expression in human neutrophils. *Nat.*
762 *Commun.*, **6**, 7545.
- 763 12. Nica,A.C., Parts,L., Glass,D., Nisbet,J., Barrett,A., Sekowska,M., Travers,M., Potter,S.,
764 Grundberg,E., Small,K., *et al.* (2011) The architecture of gene regulatory variation
765 across multiple human tissues: the MuTHER study. *PLoS Genet.*, **7**, e1002003.
- 766 13. Myers,A.J., Gibbs,J.R., Webster,J. a, Rohrer,K., Zhao,A., Marlowe,L., Kaleem,M.,
767 Leung,D., Bryden,L., Nath,P., *et al.* (2007) A survey of genetic human cortical gene
768 expression. *Nat. Genet.*, **39**, 1494–9.
- 769 14. Field,J.M., Hazinski,M.F., Sayre,M.R., Chameides,L., Schexnayder,S.M., Hemphill,R.,
770 Samson,R. a., Kattwinkel,J., Berg,R. a., Bhanji,F., *et al.* (2010) Part 1: Executive
771 summary: 2010 American Heart Association Guidelines for Cardiopulmonary
772 Resuscitation and Emergency Cardiovascular Care. *Circulation*, **122**, 640–657.
- 773 15. Emilsson,V., Thorleifsson,G., Zhang,B., Leonardson,A.S., Zink,F., Zhu,J., Carlson,S.,
774 Helgason,A., Walters,G.B., Gunnarsdottir,S., *et al.* (2008) Genetics of gene expression
775 and its effect on disease. **452**.

- 776 16. Schadt,E.E., Molony,C., Chudin,E., Hao,K., Yang,X., Lum,P.Y., Kasarskis,A., Zhang,B.,
777 Wang,S., Suver,C., *et al.* (2008) Mapping the genetic architecture of gene expression in
778 human liver. *PLoS Biol.*, **6**, e107.
- 779 17. Hao,K., Bossé,Y., Nickle,D.C., Paré,P.D., Postma,D.S., Laviolette,M., Sandford,A.,
780 Hackett,T.L., Daley,D., Hogg,J.C., *et al.* (2012) Lung eQTLs to help reveal the
781 molecular underpinnings of asthma. *PLoS Genet.*, **8**, e1003029.
- 782 18. Li,Q., Seo,J.H., Stranger,B., McKenna,A., Pe'Er,I., Laframboise,T., Brown,M.,
783 Tyekucheva,S. and Freedman,M.L. (2013) Integrative eQTL-based analyses reveal the
784 biology of breast cancer risk loci. *Cell*, **152**, 633–641.
- 785 19. Ongen,H., Andersen,C.L., Bramsen,J.B., Oster,B., Rasmussen,M.H., Ferreira,P.G.,
786 Sandoval,J., Vidal,E., Whiffin,N., Planchon,A., *et al.* (2014) Putative cis-regulatory
787 drivers in colorectal cancer. *Nature*, **512**, 87–90.
- 788 20. Zou,F., Chai,H.S., Younkin,C.S., Allen,M., Crook,J., Pankratz,V.S., Carrasquillo,M.M.,
789 Rowley,C.N., Nair,A.A., Middha,S., *et al.* (2012) Brain expression genome-wide
790 association study (eGWAS) identifies human disease-associated variants. *PLoS*
791 *Genet.*, **8**, e1002707.
- 792 21. Albert,F.W. and Kruglyak,L. (2015) The role of regulatory variation in complex traits and
793 disease. *Nat. Rev. Genet.*, **16**, 197–212.
- 794 22. Gibson,G., Powell,J.E. and Marigorta,U.M. (2015) Expression quantitative trait locus
795 analysis for translational medicine. *Genome Med.*, **7**, 60.
- 796 23. Barreiro,L., Tailleux,L., Pai,A., Gicquel,B., Marioni,J.C. and Gilad,Y. (2012) Deciphering
797 the genetic architecture of variation in the immune response to Mycobacterium
798 tuberculosis infection. *Proc. Natl. Acad. Sci.*, **109**, 1204–1209.
- 799 24. Fairfax,B.P., Humburg,P., Makino,S., Naranbhai,V., Wong,D., Lau,E., Jostins,L.,

- 800 Plant,K., Andrews,R., McGee,C., *et al.* (2014) Innate Immune Activity Conditions the
801 Effect of Regulatory Variants upon Monocyte Gene Expression. *Science (80-.)*, **343**,
802 1246949–1246949.
- 803 25. Marioni,J.C., Mason,C.E., Mane,S.M., Stephens,M. and Gilad,Y. (2008) RNA-seq: An
804 assessment of technical reproducibility and comparison with gene expression arrays.
805 10.1101/gr.079558.108.
- 806 26. Zhang,X., Johnson,A.D., Hendricks,A.E., Hwang,S.-J., Tanriverdi,K., Ganesh,S.K.,
807 Smith,N.L., Peyser,P.A., Freedman,J.E. and O'Donnell,C.J. (2014) Genetic
808 associations with expression for genes implicated in GWAS studies for atherosclerotic
809 cardiovascular disease and blood phenotypes. *Hum. Mol. Genet.*, **23**, 782–795.
- 810 27. Zhang,X., Joehanes,R., Chen,B.H., Huan,T., Ying,S., Munson,P.J., Johnson,A.D.,
811 Levy,D. and O'Donnell,C.J. (2015) Identification of common genetic variants controlling
812 transcript isoform variation in human whole blood. *Nat. Genet.*, **47**, 345–352.
- 813 28. Zhao,S., Fung-Leung,W.-P., Bittner,A., Ngo,K. and Liu,X. (2014) Comparison of RNA-
814 Seq and microarray in transcriptome profiling of activated T cells. *PLoS One*, **9**,
815 e78644.
- 816 29. Majewski,J. and Pastinen,T. (2011) The study of eQTL variations by RNA-seq: from
817 SNPs to phenotypes. *Trends Genet.*, **27**, 72–79.
- 818 30. Russo,G., Zegar,C. and Giordano,A. (2003) Advantages and limitations of microarray
819 technology in human cancer. *Oncogene*, **22**, 6497–6507.
- 820 31. Sun,W. and Hu,Y. (2013) eQTL Mapping Using RNA-seq Data. *Stat. Biosci.*, **5**, 198–219.
- 821 32. 't Hoen,P. a C., Friedländer,M.R., Almlöf,J., Sammeth,M., Pulyakhina,I., Anvar,S.Y.,
822 Laros,J.F.J., Buermans,H.P.J., Karlberg,O., Brännvall,M., *et al.* (2013) Reproducibility
823 of high-throughput mRNA and small RNA sequencing across laboratories. *Nat.*

- 824 *Biotechnol.*, **31**, 1015–22.
- 825 33. Pickrell, J.K., Marioni, J.C., Pai, A.A., Degner, J.F., Engelhardt, B.E., Nkadori, E.,
826 Veyrieras, J.-B., Stephens, M., Gilad, Y. and Pritchard, J.K. (2010) Understanding
827 mechanisms underlying human gene expression variation with RNA sequencing.
828 *Nature*, **464**, 768–772.
- 829 34. Montgomery, S.B., Sammeth, M., Gutierrez-Arcelus, M., Lach, R.P., Ingle, C., Nisbett, J.,
830 Guigo, R. and Dermitzakis, E.T. (2010) Transcriptome genetics using second generation
831 sequencing in a Caucasian population. *Nature*, **464**, 773–777.
- 832 35. Lappalainen, T., Sammeth, M., Friedländer, M.R., 't Hoen, P. a C., Monlong, J., Rivas, M. a,
833 González-Porta, M., Kurbatova, N., Griebel, T., Ferreira, P.G., *et al.* (2013) Transcriptome
834 and genome sequencing uncovers functional variation in humans. *Nature*, **501**, 506–11.
- 835 36. Battle, A., Mostafavi, S., Zhu, X., Potash, J.B., Weissman, M.M., McCormick, C.,
836 Haudenschild, C.D., Beckman, K.B., Shi, J., Mei, R., *et al.* (2014) Characterizing the
837 genetic basis of transcriptome diversity through RNA-sequencing of 922 individuals.
838 *Genome Res.*, **24**, 14–24.
- 839 37. Lalonde, E., Ha, K.C.H., Wang, Z., Bemmo, A., Kleinman, C.L., Kwan, T., Pastinen, T. and
840 Majewski, J. (2011) RNA sequencing reveals the role of splicing polymorphisms in
841 regulating human gene expression. *Genome Res*, 10.1101/gr.111211.110.21.
- 842 38. Kumar, V., Westra, H.-J., Karjalainen, J., Zhernakova, D. V., Esko, T., Hrdlickova, B.,
843 Almeida, R., Zhernakova, A., Reinmaa, E., Vösa, U., *et al.* (2013) Human Disease-
844 Associated Genetic Variation Impacts Large Intergenic Non-Coding RNA Expression.
845 *PLoS Genet.*, **9**, e1003201.
- 846 39. Buil, A., Brown, A.A., Lappalainen, T., Viñuela, A., Davies, M.N., Zheng, H.-F.,
847 Richards, J.B., Glass, D., Small, K.S., Durbin, R., *et al.* (2014) Gene-gene and gene-
848 environment interactions detected by transcriptome sequence analysis in twins. *Nat.*

- 849 *Genet.*, **47**, 88–91.
- 850 40. Conde,L., Bracci,P.M., Richardson,R., Montgomery,S.B. and Skibola,C.F. (2013)
- 851 Integrating GWAS and Expression Data for Functional Characterization of Disease-
- 852 Associated SNPs: An Application to Follicular Lymphoma. *Am. J. Hum. Genet.*, **92**,
- 853 126–130.
- 854 41. Simon,L.M., Chen,E.S., Edelstein,L.C., Kong,X., Bhatlekar,S., Rigoutsos,I., Bray,P.F.
- 855 and Shaw,C.A. (2016) Integrative Multi-omic Analysis of Human Platelet eQTLs
- 856 Reveals Alternative Start Site in Mitofusin 2. *Am. J. Hum. Genet.*,
- 857 10.1016/j.ajhg.2016.03.007.
- 858 42. Li,H., Pouladi,N., Achour,I., Gardeux,V., Li,J., Li,Q., Zhang,H.H., Martinez,F.D., Skip
- 859 Garcia,J.G.N. and Lussier,Y.A. (2015) eQTL networks unveil enriched mRNA master
- 860 integrators downstream of complex disease-associated SNPs. *J. Biomed. Inform.*, **58**,
- 861 226–234.
- 862 43. Huang,L., Xu,W., Yan,D., Dai,L. and Shi,X. (2016) Identification of expression
- 863 quantitative trait loci of RPTOR for susceptibility to glioma. *Tumor Biol.*, **37**, 2305–2311.
- 864 44. Jeong,S., Patel,N., Edlund,C.K., Hartiala,J., Hazelett,D.J., Itakura,T., Wu,P.C.,
- 865 Avery,R.L., Davis,J.L., Flynn,H.W., *et al.* (2015) Identification of a novel mucin gene
- 866 HCG22 associated with steroid-induced ocular hypertension. *Investig. Ophthalmol. Vis.*
- 867 *Sci.*, **56**, 2737–2748.
- 868 45. Moffatt,M.F., Kabesch,M., Liang,L., Dixon,A.L., Strachan,D., Heath,S., Depner,M., von
- 869 Berg,A., Bufe,A., Rietschel,E., *et al.* (2007) Genetic variants regulating ORMDL3
- 870 expression contribute to the risk of childhood asthma. *Nature*, **448**, 470–473.
- 871 46. Barrett,J.C., Hansoul,S., Nicolae,D.L., Cho,J.H., Duerr,R.H., Rioux,J.D., Brant,S.R.,
- 872 Silverberg,M.S., Taylor,K.D., Barmada,M.M., *et al.* (2008) Genome-wide association
- 873 defines more than 30 distinct susceptibility loci for Crohn's disease. *Nat. Genet.*, **40**,

874 955–962.

875 47. Li,X., Hastie,A.T., Hawkins,G. a., Moore,W.C., Ampleford,E.J., Milosevic,J., Li,H.,
876 Busse,W.W., Erzurum,S.C., Kaminski,N., *et al.* (2015) eQTL of bronchial epithelial cells
877 and bronchial alveolar lavage deciphers GWAS-identified asthma genes. *Allergy*, **70**,
878 n/a–n/a.

879 48. Nica,A.C., Montgomery,S.B., Dimas,A.S., Stranger,B.E., Beazley,C., Barroso,I. and
880 Dermitzakis,E.T. (2010) Candidate causal regulatory effects by integration of
881 expression QTLs with complex trait genetic associations. *PLoS Genet.*, **6**, e1000895.

882 49. Veyrieras,J.-B., Kudravalli,S., Kim,S.Y., Dermitzakis,E.T., Gilad,Y., Stephens,M. and
883 Pritchard,J.K. (2008) High-Resolution Mapping of Expression-QTLs Yields Insight into
884 Human Gene Regulation. *PLoS Genet.*, **4**, e1000214.

885 50. Yang,T.-P., Beazley,C., Montgomery,S.B., Dimas,A.S., Gutierrez-Arcelus,M.,
886 Stranger,B.E., Deloukas,P. and Dermitzakis,E.T. (2010) Genevar: a database and Java
887 application for the analysis and visualization of SNP-gene associations in eQTL studies.
888 *Bioinformatics*, **26**, 2474–2476.

889 51. The GTEx Consortium (2013) The Genotype-Tissue Expression (GTEx) project. *Nat.*
890 *Genet.*, **45**, 580–5.

891 52. Harley,I.T.W., Kaufman,K.M., Langefeld,C.D., Harley,J.B. and Kelly,J.A. (2009) Genetic
892 susceptibility to SLE: new insights from fine mapping and genome-wide association
893 studies. *Nat. Rev. Genet.*, **10**, 285–90.

894 53. Cui,Y., Sheng,Y. and Zhang,X. (2013) Genetic susceptibility to SLE: Recent progress
895 from GWAS. *J. Autoimmun.*, **41**, 25–33.

896 54. Deng,Y. and Tsao,B.P. (2014) Advances in lupus genetics and epigenetics. *Curr. Opin.*
897 *Rheumatol.*, **26**, 1–11.

- 898 55. Yang, J., Lee, S.H., Goddard, M.E. and Visscher, P.M. (2011) GCTA: A Tool for Genome-
899 wide Complex Trait Analysis. *Am. J. Hum. Genet.*, **88**, 76–82.
- 900 56. Giambartolomei, C., Vukcevic, D., Schadt, E.E., Franke, L., Hingorani, A.D., Wallace, C. and
901 Plagnol, V. (2014) Bayesian Test for Colocalisation between Pairs of Genetic
902 Association Studies Using Summary Statistics. *PLoS Genet.*, **10**, e1004383.
- 903 57. Kozyrev, S. V., Abelson, A.-K., Wojcik, J., Zaghlool, A., Linga Reddy, M.V.P., Sanchez, E.,
904 Gunnarsson, I., Svenungsson, E., Sturfelt, G., Jönsen, A., *et al.* (2008) Functional variants
905 in the B-cell gene BANK1 are associated with systemic lupus erythematosus. *Nat.*
906 *Genet.*, **40**, 211–216.
- 907 58. Lewis, M.J., Vyse, S., Shields, A.M., Boeltz, S., Gordon, P.A., Spector, T.D., Lehner, P.J.,
908 Walczak, H. and Vyse, T.J. (2015) UBE2L3 polymorphism amplifies NF- κ B activation
909 and promotes plasma cell development, linking linear ubiquitination to multiple
910 autoimmune diseases. *Am. J. Hum. Genet.*, **96**, 221–234.
- 911 59. Noble, J.A., White, A.M., Lazzeroni, L.C., Valdes, A.M., Mirel, D.B., Reynolds, R., Grupe, A.,
912 Aud, D., Peltz, G. and Erlich, H.A. Associated With Type 1 Diabetes. **06**, 1579–1582.
- 913 60. Liu, Y., Wang, X., Cheng, X., Lu, Y. and Wang, G. (2015) Skp1 in lung cancer: Clinical
914 significance and therapeutic efficacy of its small molecule inhibitors. **6**.
- 915 61. Wu, J.Q., Seay, M., Schulz, V.P., Hariharan, M., Tuck, D., Lian, J., Du, J., Shi, M., Ye, Z.,
916 Gerstein, M., *et al.* (2012) Tcf7 is an important regulator of the switch of self-renewal
917 and differentiation in a multipotential hematopoietic cell line. *PLoS Genet.*, **8**.
- 918 62. Zhou, W., Wei, W. and Sun, Y. (2013) Genetically engineered mouse models for functional
919 studies of SKP1-CUL1-F-box-protein (SCF) E3 ubiquitin ligases. *Cell Res*, **23**, 599–
920 619.
- 921 63. Bentham, J., Morris, D.L., Cunninghame Graham, D.S., Pinder, C.L., Tomblinson, P.,

- 922 Behrens,T.W., Martín,J., Fairfax,B.P., Knight,J.C., Chen,L., *et al.* (2015) Genetic
923 association analyses implicate aberrant regulation of innate and adaptive immunity
924 genes in the pathogenesis of systemic lupus erythematosus. *Nat. Genet.*,
925 10.1038/ng.3434.
- 926 64. Westra,H.-J., Peters,M.J., Esko,T., Yaghoobkar,H., Schurmann,C., Kettunen,J.,
927 Christiansen,M.W., Fairfax,B.P., Schramm,K., Powell,J.E., *et al.* (2013) Systematic
928 identification of trans eQTLs as putative drivers of known disease associations. *Nat.*
929 *Genet.*, **45**, 1238–43.
- 930 65. Ward,L.D. and Kellis,M. (2012) HaploReg: A resource for exploring chromatin states,
931 conservation, and regulatory motif alterations within sets of genetically linked variants.
932 *Nucleic Acids Res.*, **40**, 930–934.
- 933 66. Salloum,R., Franek,B.S., Kariuki,S.N., Rhee,L., Mikolaitis,R. a., Jolly,M., Utset,T.O. and
934 Niewold,T.B. (2010) Genetic variation at the IRF7/PHRF1 locus is associated with
935 autoantibody profile and serum interferon-alpha activity in lupus patients. *Arthritis*
936 *Rheum.*, **62**, 553–561.
- 937 67. Wang,T.J., Zhang,F., Richards,J.B., Kestenbaum,B., van Meurs,J.B., Berry,D., Kiel,D.P.,
938 Streeten,E.A., Ohlsson,C., Koller,D.L., *et al.* (2010) Common genetic determinants of
939 vitamin D insufficiency: a genome-wide association study. *Lancet*, **376**, 180–188.
- 940 68. Yap,K.S., Northcott,M., Hoi, a. B.-Y., Morand,E. and Nikpour,M. (2015) Association of
941 low vitamin D with high disease activity in an Australian systemic lupus erythematosus
942 cohort. *Lupus Sci. Med.*, **2**, e000064–e000064.
- 943 69. Wassif,C. a, Zhu,P., Kratz,L., Krakowiak,P. a, Battaile,K.P., Weight,F.F., Grinberg,A.,
944 Steiner,R.D., Nwokoro,N.A., Kelley,R.I., *et al.* (2001) Biochemical, phenotypic and
945 neurophysiological characterization of a genetic mouse model of RSH/Smith--Lemli--
946 Opitz syndrome. *Hum. Mol. Genet.*, **10**, 555–564.

- 947 70. Shah,D., Mahajan,N., Sah,S., Nath,S.K. and Paudyal,B. (2014) Oxidative stress and its
948 biomarkers in systemic lupus erythematosus. *J. Biomed. Sci.*, **21**, 23.
- 949 71. Luo,X., Yang,W., Ye,D.-Q., Cui,H., Zhang,Y., Hirankarn,N., Qian,X., Tang,Y., Lau,Y.L.,
950 de Vries,N., *et al.* (2011) A functional variant in microRNA-146a promoter modulates its
951 expression and confers disease risk for systemic lupus erythematosus. *PLoS Genet.*, **7**,
952 e1002128.
- 953 72. Hom,G., Ph,D., Graham,R.R., Modrek,B., Taylor,K.E., Ortmann,W., Garnier,S., Lee,A.T.,
954 Chung,S.A., Ferreira,R.C., *et al.* (2008) Association of Systemic Lupus Erythematosus
955 with. *Genetics*.
- 956 73. Guthridge,J.M., Lu,R., Sun,H., Sun,C., Wiley,G.B., Dominguez,N., MacWana,S.R.,
957 Lessard,C.J., Kim-Howard,X., Cobb,B.L., *et al.* (2014) Two functional lupus-associated
958 BLK promoter variants control cell-type- and developmental-stage-specific transcription.
959 *Am. J. Hum. Genet.*, **94**, 586–598.
- 960 74. Kim,H., Barnitz,R.A., Kreslavsky,T., Brown,F.D., Moffett,H., Lemieux,M.E., Kaygusuz,Y.,
961 Meissner,T., Holderried,T.A.W., Chan,S., *et al.* (2009) egulatory T cells (CD4 and CD8
962 T.
- 963 75. Baine,I., Basu,S., Ames,R., Sellers,R.S. and Macian,F. (2013) Helios induces epigenetic
964 silencing of IL2 gene expression in regulatory T cells. *J. Immunol.*, **190**, 1008–16.
- 965 76. Getnet,D., Grosso,J.F., Goldberg,M. V., Harris,T.J., Yen,H.R., Bruno,T.C., Durham,N.M.,
966 Hipkiss,E.L., Pyle,K.J., Wada,S., *et al.* (2010) A role for the transcription factor Helios in
967 human CD4+CD25+ regulatory T cells. *Mol. Immunol.*, **47**, 1595–1600.
- 968 77. Isakson,P., Holland,P. and Simonsen,A. (2013) The role of ALFY in selective autophagy.
969 *Cell Death Differ.*, **20**, 12–20.
- 970 78. Yang,W., Shen,N., Ye,D.Q., Liu,Q., Zhang,Y., Qian,X.X., Hirankarn,N., Ying,D.,

- 971 Pan,H.F., Mok,C.C., *et al.* (2010) Genome-wide association study in asian populations
972 identifies variants in ETS1 and WDFY4 associated with systemic lupus erythematosus.
973 *PLoS Genet.*, **6**.
- 974 79. McLaren,W., Pritchard,B., Rios,D., Chen,Y., Flicek,P. and Cunningham,F. (2010)
975 Deriving the consequences of genomic variants with the Ensembl API and SNP Effect
976 Predictor. *Bioinformatics*, **26**, 2069–2070.
- 977 80. Graham,R.R., Kozyrev,S. V, Baechler,E.C., Reddy,M.V.P.L., Plenge,R.M., Bauer,J.W.,
978 Ortmann,W. a, Koeuth,T., González Escribano,M.F., Pons-Estel,B., *et al.* (2006) A
979 common haplotype of interferon regulatory factor 5 (IRF5) regulates splicing and
980 expression and is associated with increased risk of systemic lupus erythematosus. *Nat.*
981 *Genet.*, **38**, 550–555.
- 982 81. Graham,R.R., Kyogoku,C., Sigurdsson,S., Vlasova,I.A., Davies,L.R.L., Baechler,E.C.,
983 Plenge,R.M., Koeuth,T., Ortmann,W.A., Hom,G., *et al.* (2007) Three functional variants
984 of IFN regulatory factor 5 (IRF5) define risk and protective haplotypes for human lupus.
985 *Proc. Natl. Acad. Sci. U. S. A.*, **104**, 6758–63.
- 986 82. Lappalainen,T. (2015) Functional genomics bridges the gap between quantitative
987 genetics and molecular biology. *Genome Res.*, **25**, 1427–1431.
- 988 83. Battle, a. and Montgomery,S.B. (2014) Determining causality and consequence of
989 expression quantitative trait loci. *Hum. Genet.*, **133**, 727–735.
- 990 84. Jäger,R., Migliorini,G., Henrion,M., Kandaswamy,R., Speedy,H.E., Heindl,A., Whiffin,N.,
991 Carnicer,M.J., Broome,L., Dryden,N., *et al.* (2015) Capture Hi-C identifies the chromatin
992 interactome of colorectal cancer risk loci. *Nat. Commun.*, **6**, 6178.
- 993 85. Zhao,Z., Tavoosidana,G., Sjölander,M., Göndör,A., Mariano,P., Wang,S., Kanduri,C.,
994 Lezcano,M., Sandhu,K.S., Singh,U., *et al.* (2006) Circular chromosome conformation
995 capture (4C) uncovers extensive networks of epigenetically regulated intra- and

- 996 interchromosomal interactions. *Nat. Genet.*, **38**, 1341–1347.
- 997 86. Kelsell,D.P., Norgett,E.E., Unsworth,H., Teh,M.-T., Cullup,T., Mein,C.A., Dopping-
998 Hepenstal,P.J., Dale,B.A., Tadini,G., Fleckman,P., *et al.* (2005) Mutations in ABCA12
999 underlie the severe congenital skin disease harlequin ichthyosis. *Am. J. Hum. Genet.*,
1000 **76**, 794–803.
- 1001 87. Steidl,U., Steidl,C., Ebralidze,A., Chapuy,B., Han,H., Will,B., Rosenbauer,F., Becker,A.,
1002 Wagner,K., Koschmieder,S., *et al.* (2007) A distal single nucleotide polymorphism alters
1003 long-range regulation of the PU . 1 gene in acute myeloid leukemia. *J. Clin. Invest.*,
1004 **117**, 2611–2620.
- 1005 88. Freedman,M.L., Monteiro,A.N.A., Gayther,S.A., Coetzee,G.A., Risch,A., Plass,C.,
1006 Casey,G., De Biasi,M., Carlson,C., Duggan,D., *et al.* (2011) Principles for the post-
1007 GWAS functional characterization of cancer risk loci. *Nat. Genet.*, **43**, 513–518.
- 1008 89. Graveley,B.R. (2008) The haplo-spliceo-transcriptome: common variations in alternative
1009 splicing in the human population. *Trends Genet.*, **24**, 5–7.
- 1010 90. Wang,G.-S. and Cooper,T.A. (2007) Splicing in disease: disruption of the splicing code
1011 and the decoding machinery. *Nat. Rev. Genet.*, **8**, 749–761.
- 1012 91. Li,Y.I., van de Geijn,B., Raj,A., Knowles,D.A., Petti,A.A., Golan,D., Gilad,Y. and
1013 Pritchard,J.K. (2016) RNA splicing is a primary link between genetic variation and
1014 disease. *Science*, **352**, 600–4.
- 1015 92. Wang,J.H., Avitahl,N., Cariappa,A., Friedrich,C., Ikeda,T., Renold,A., Andrikopoulos,K.,
1016 Liang,L., Pillai,S., Morgan,B.A., *et al.* (1998) Aiolos regulates B cell activation and
1017 maturation to effector state. *Immunity*, **9**, 543–553.
- 1018 93. Shabalina,A.A. (2012) Matrix eQTL: ultra fast eQTL analysis via large matrix operations.
1019 *Bioinformatics*, **28**, 1353–1358.

- 1020 94. Zheng,X., Levine,D., Shen,J., Gogarten,S.M., Laurie,C. and Weir,B.S. (2012) A high-
1021 performance computing toolset for relatedness and principal component analysis of
1022 SNP data. *Bioinformatics*, **28**, 3326–3328.
- 1023 95. Li,H., Handsaker,B., Wysoker,A., Fennell,T., Ruan,J., Homer,N., Marth,G., Abecasis,G.,
1024 Durbin,R. and Subgroup,1000 Genome Project Data Processing (2009) The Sequence
1025 Alignment/Map format and SAMtools. *Bioinformatics*, **25**, 2078–2079.
- 1026 96. Ongen,H. and Dermitzakis,E.T. (2015) Alternative Splicing QTLs in European and
1027 African Populations. *Am. J. Hum. Genet.*, **97**, 567–575.
- 1028 97. Pruim,R.J., Welch,R.P., Sanna,S., Teslovich,T.M., Chines,P.S., Gliedt,T.P., Boehnke,M.,
1029 Abecasis,G.R. and Willer,C.J. (2010) LocusZoom: Regional visualization of genome-
1030 wide association scan results. *Bioinformatics*, **26**, 2336–2337.
- 1031 98. Cunningham,F., Amode,M.R., Barrell,D., Beal,K., Billis,K., Brent,S., Carvalho-Silva,D.,
1032 Clapham,P., Coates,G., Fitzgerald,S., *et al.* (2015) Ensembl 2015. *Nucleic Acids Res.*,
1033 **43**, D662–D669.
- 1034 99. Kent,W.J., Sugnet,C.W., Furey,T.S. and Roskin,K.M. (1976) The Human Genome
1035 Browser at UCSC W. *J. Med. Chem.*, **19**, 1228–31.
- 1036

1037 **Legends to figures**

1038 **Fig. 1: Two-stage *cis*-eQTL annotation pipeline for SLE susceptibility loci.**

1039 SLE susceptibility variants (**Table 1**) were annotated using residualized expression or
1040 summary-level eQTL statistics from three expression datasets: microarray probe-level
1041 expression data, and both gene-level and exon-level RNA-Seq quantifications. Each
1042 expression dataset was generated from LCLs from individuals of the TwinsUK cohort. **A)** We
1043 undertook *cis*-eQTL analysis of +/-1Mb intervals around each SNP and associations with
1044 $q < 0.05$ after FDR adjustment were taken forward. **B)** Summary-level data from significant
1045 *cis*-eQTLs were tested for evidence of a shared causal variant using firstly conditional
1046 analysis using the TwinsUK genetic data as a reference panel, then colocalisation analysis
1047 to test for a single causal variant common to both traits. Associations passing these
1048 thresholds (described fully in methods) were classified as candidate-causal eQTLs and
1049 eGenes. Summary results per quantification type for significant and candidate-causal
1050 associations are shown in **Table 3** for microarray, **Table 4** for RNA-Seq (gene-level), and
1051 **Table 5** for RNA-Seq (exon-level). Full summary results are available in **Table S1, S2,** and
1052 **S3** respectively.

1053

1054 **Fig. 2: Candidate-causal eQTLs and eGenes detected across quantification types.**

1055 Candidate-causal eQTLs and eGenes detected using microarray (probe-level), RNA-Seq
1056 (gene-level), and RNA-Seq (exon-level) quantifications from the TwinsUK datasets are
1057 represented in their genomic context (**Tables 3, 4,** and **5** respectively). Only chromosomes
1058 harbouring one or more candidate-causal eQTL or eGene per quantification type are shown.

1059

1060 **Fig. 3: RNA-Seq gene-level and exon-level analysis implicate *NADSYN1* as a novel** 1061 **candidate-causal eGene.**

1062 **A)** *Cis*-eQTL analysis of GWAS SNP rs3794060 reveals the risk variant [C] leads to
1063 substantial down-regulation at the gene-level of novel susceptibility gene *NADSYN1* in the
1064 TwinsUK cohort that was not detected using microarray. **B)** The same analysis using exon-
1065 level quantification leads to the inference of the gene-level effect being driven by
1066 considerable expression disruption of two meta-exons of *NADSYN1* (meta-exon 11 and
1067 meta-exon 12). Association *P*-values of rs3794060 against exon quantifications are plotted
1068 with reference to the specific exon in the collapsed-gene model of *NADSYN1* (all annotated
1069 transcripts combined).

1070

1071 **Fig. 4: Non-coding candidate-causal eGenes detected using exon-level RNA-Seq.**

1072 The three figures denote the eQTLs and corresponding non-coding eGenes identified from
1073 *cis*-eQTL analysis of GWAS SNPs against TwinsUK exon-level quantifications in LCLs. The
1074 top panels display the signal from the GWAS association plotted as $-\log_{10}(P)$, below which
1075 the exon-level eQTL *P*-values for the effects showing colocalisation with the GWAS signal
1076 are illustrated. The bar across the middle of the figure denotes the boundaries of the eQTL,
1077 below which there is a panel showing the association *P*-value of the GWAS SNP against the
1078 candidate-causal non-coding exons. The bottom panel shows LCL RNA-Seq alignments
1079 from ENCODE to show that the regions containing the candidate-causal eQTLs are
1080 expressed. **A)** GWAS SNP rs2431697 is a candidate-causal eQTL for non-coding eGene
1081 *MIR146A*. **B)** GWAS SNP rs2736340 is a candidate-causal eQTL for non-coding eGenes
1082 *RP11-148O21.4* and *RP11-148O21.2*. **C)** GWAS SNP rs3794060 is a candidate-causal
1083 eQTL for non-coding eGene *RP11-660L16.2*.

1084

1085

1086

1087 **Fig. 5: Identification of novel eGene *IKZF2* and potential causal mechanism using**
1088 **RNA-Seq splice-junction quantification.**

1089 *Cis*-asQTL analysis of GWAS SNP rs3768792 against splice-junction quantifications
1090 classified *IKZF2* as a candidate-causal eGene with risk variant [G] causing upregulation of
1091 the exon 6A–exon 6B junction that is unique to truncated isoform ENST00000413091. **A)**
1092 GWAS association signal across the *IKZF2* locus (chr2q34), tagged by rs3768792 localised
1093 in the 3'-UTR of *IKZF2*. *Cis*-asQTL association signal of rs3768792 against splice-junction
1094 quantification of exon 6A–exon 6B shows significance and colocalisation with the GWAS
1095 signal. **B)** The exon 6A–exon 6B junction is unique to truncated isoform ENST00000413091.
1096 Exon 6B harbours a premature stop-codon and therefore is not translated into the full-length
1097 protein that contains the dimerization domains in exon 8. **C)** Close-up of the exon 6A–exon
1098 6B junction and association ($P=3.80E^{-05}$) with GWAS SNP rs3768792. A potential causal
1099 asQTL in near-perfect LD was identified that is located within the polypyrimidine tract of the
1100 junction and may induce splicing (rs2291241, $P=1.70E^{-05}$).

1101

1102 **Fig. 6: Identification of potential disease-associated mechanisms at the *WDFY4***
1103 **susceptibility locus using asQTL mapping.**

1104 **A)** Our SLE GWAS indicates *WDFY4* as the candidate gene at the chr10q11.23 locus
1105 tagged by intronic variant rs2663052, as well as the missense coding variant rs7097397 in
1106 exon 31 that is in strong LD. *Cis*-eQTL showed rs2663052 is correlated with upregulation of
1107 the exon 34A–34B junction of *WDFY4* (signal is colocalised with GWAS) that is unique to the
1108 short isoform (ENST00000374161). This isoform lacks the two enzymatic WD40 domains of
1109 the full length isoform (ENST00000325239). **B)** Two potential functional mechanisms may
1110 occur when harbouring the risk haplotype that carries both risk alleles. Firstly an Arg to Gln
1111 amino-acid substitution by rs7097397 in exon 31 that is shared by both the canonical and
1112 short isoforms of *WDFY4*, and secondly an upregulation of the short isoform ($P=3.31E^{-19}$)

1113 that lacks functional domains, caused by rs2663052 or correlated variants, with
1114 corresponding down-regulation of the full-length isoform ($P=3.01^{E-06}$).

1115

1116 **Fig. 7: Heatmap of candidate-causal eQTLs and eGenes detected across all**
1117 **expression-quantification types.**

1118 Heatmap of all candidate-causal *cis*-eQTL associations across the four quantification types
1119 (microarray, RNA-Seq gene-level, RNA-Seq exon-level, and RNA-Seq splice-junction level).
1120 The first column is the key showing the relative P value of the eQTLs within each platform.
1121 For the platform-specific columns, if an eQTL-eGene association is candidate-causal in at
1122 least one quantification type, the data is displayed across all platforms. Rows are ordered
1123 by decreasing cumulative significance across quantification types. To normalize across
1124 quantification types, relative significance of each association per column was calculated as
1125 the $-\log_2 (P/P_{\max})$; where P_{\max} is the most significant association per quantification type. If an
1126 association is deemed to be candidate-causal within a particular profiling-type, it is
1127 highlighted with an asterisk.

1128 **Supporting Information**

1129 **S1 Table. All significant eQTLs ($q < 0.05$) and associated eGenes detected at**
1130 **microarray (probe-level) with conditional and colocalisation results.**

1131 **S2 Table. All significant eQTLs ($q < 0.05$) and associated eGenes detected at RNA-Seq**
1132 **(gene-level) with conditional and colocalisation results.**

1133 **S3 Table. All significant eQTLs ($q < 0.05$) and associated eGenes detected at RNA-Seq**
1134 **(exon-level) with conditional and colocalisation results.**

1135 **S1 Fig. Number of eQTL discoveries per quantification type.** Including significant
1136 associations ($q < 0.05$), and candidate-causal associations (significant, and not-independent
1137 and colocalised with GWAS).

1138 **S2 Fig. Number of eGene discoveries per quantification type.** Including significant
1139 associations ($q < 0.05$), and candidate-causal associations (significant, and not-independent
1140 and colocalised with GWAS).

1141 **S3 Fig. Shared candidate-causal eQTLs per quantification type.**

1142 **S4 Fig. Shared candidate-causal eGenes per quantification type.**

1143 **S5 Fig. Ratio of eQTLs to candidate-causal eGenes per quantification type.**

1144 **S6 Fig. Gene-level and exon-level candidate-causal associations with *TCF7* and *SKP1***
1145 **against rs7726414.** *Cis*-eQTL analysis at gene-level and exon-level using RNA-Seq
1146 implicate novel SLE-associated eGenes *TCF7* and *SKP1*.

1147 **S7 Fig. High gene-density over associated variants tagged by GWAS SNP rs12802200.**
1148 The six candidate-causal eGenes against rs1280220 discovered using RNA-Seq at either
1149 quantification method are marked with an asterisk.

1150 **S8 Fig. Candidate-causal eGenes *DHCR7* and *NADSYN1* for rs3794060, and non-**

1151 **coding eGene *RP11-660L16.2***. The GWAS SNP rs3794060 is a candidate-causal eGene
1152 for *DHCR7* and *NADSYN1*, and also the non-coding eGene *RP11-660L16.2* at exon-level;
1153 which is located between *DCHR7* and *NADSYN1*.

1154 **S9 Fig. Candidate-causal eGenes *FAM167A*, *BLK* and two non-coding RNAs (*RP11-*
1155 ***138021.4* and *RP11-138021.2*) driven by rs2736340**. Associated variant rs2736340 lies in
1156 a region of intense regulatory chromatin marks located in the bi-directional promoter of *BLK*
1157 and *FAM167A* which are both candidate-causal eGenes at RNA-Seq gene-level. At exon-
1158 level, the non-coding eGenes *RP11-138021.4* and *RP11-138021.2* are also candidate-
1159 causal.**

1160 **S10 Fig. Effect-size correlation of GWAS SNP associations with matched *cis*-exons**
1161 **between LCL and whole-blood.**

1162 **S4 Table. All significant eQTLs ($q < 0.05$) and associated eGenes detected at RNA-Seq**
1163 **(exon-level) | with conditional and colocalisation results in whole-blood.**

1164 **S11 Fig. Candidate-causal eQTLs and eGenes in whole blood.** Comparison with LCL
1165 associations.

1166 **S12 Fig. Whole-blood exon-level eQTL effect on *BANK1* exon 2.** Correlation between
1167 GWAS SNP and the best whole-blood eQTL for *BANK1* exon 2. Both are highly correlated
1168 with known branch-point SNP. All are weakly correlated with best LCL eQTL for *BANK1*
1169 exon 2.

1170 **S13 Fig. Exon-level eQTL analysis of *NADSYN1* in whole-blood and LCLs reveal near-**
1171 **identical splicing effect.** Meta-exons 11 and 12 are substantially disrupted with reference
1172 to GWAS SNP rs3794060 in both LCLs and whole-blood.

1173 **S5 Table. All significant asQTLs ($q < 0.05$) and associated eGenes detected at RNA-**
1174 **Seq (splice-junction level).**

1175 **S14 Fig. Proposed splicing mechanism of *NADSYN1* caused by risk haplotype tagged**
1176 **by rs3794060.** *NADSYN1* Ensembl transcript annotation displayed. *Cis*-asQTL identified the
1177 meta-exon 10 to meta-exon 12 junction is upregulated with risk allele [C] and consequently
1178 the meta-exon 11 to meta-exon 12 junction is downregulated.

1179 **S6 Table. Comparison of eQTLs and eGenes for SLE risk alleles between previously**
1180 **reported in microarray studies and from RNA-Seq in current study.**

1181 **Abbreviations**

1182 **GWAS:** Genome-Wide Association Study

1183 **eQTL:** expression Quantitative Trait Loci

1184 **RNA-Seq:** RNA-Sequencing

1185 **SLE:** Systemic Lupus Erythematosus

1186 **asQTL:** alternative-splicing Quantitative Trait Loci

1187 **SNP:** Single Nucleotide Polymorphism

1188 **LCL:** Lymphoblastoid cell line

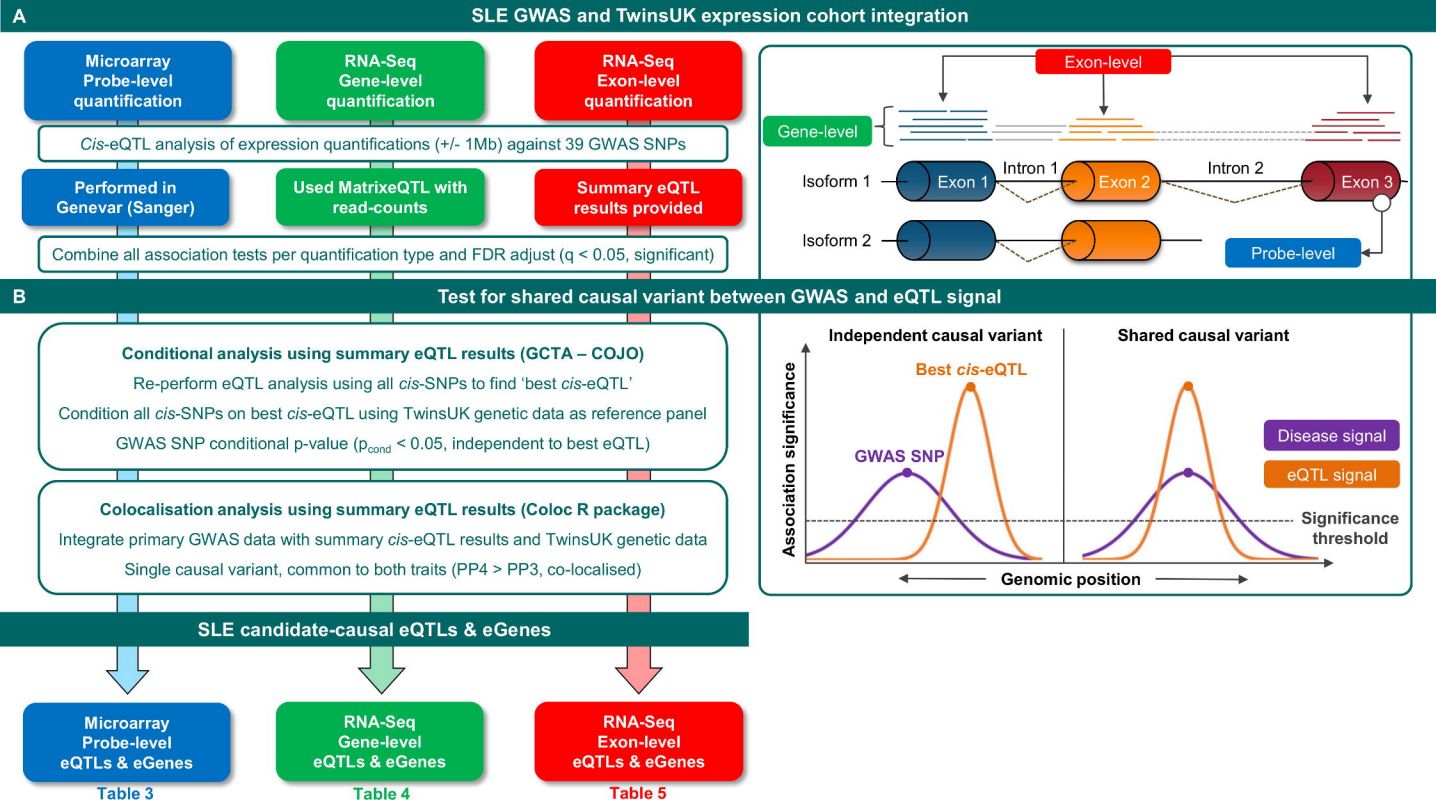


Fig 2.

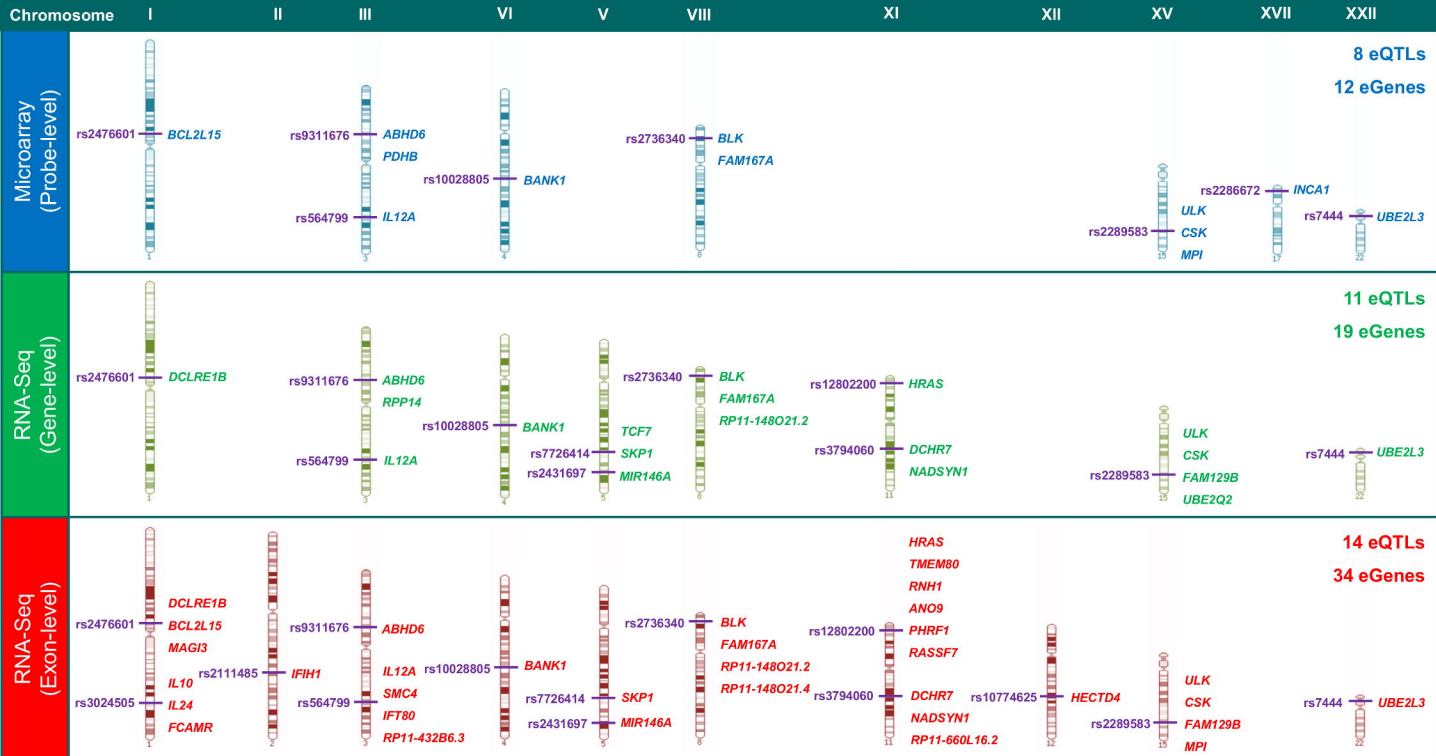


Fig 3.

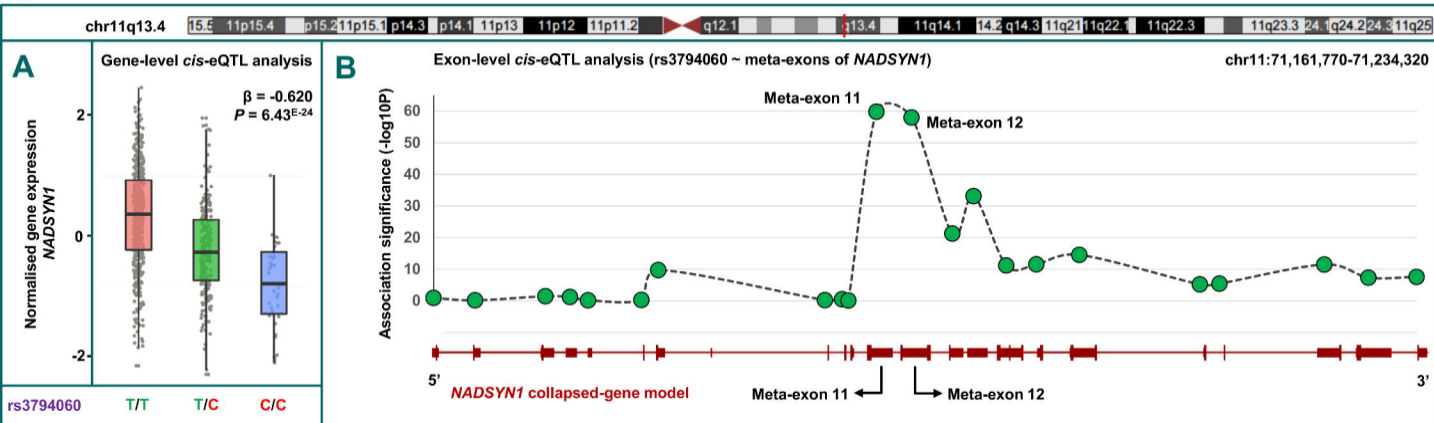


Fig 4.

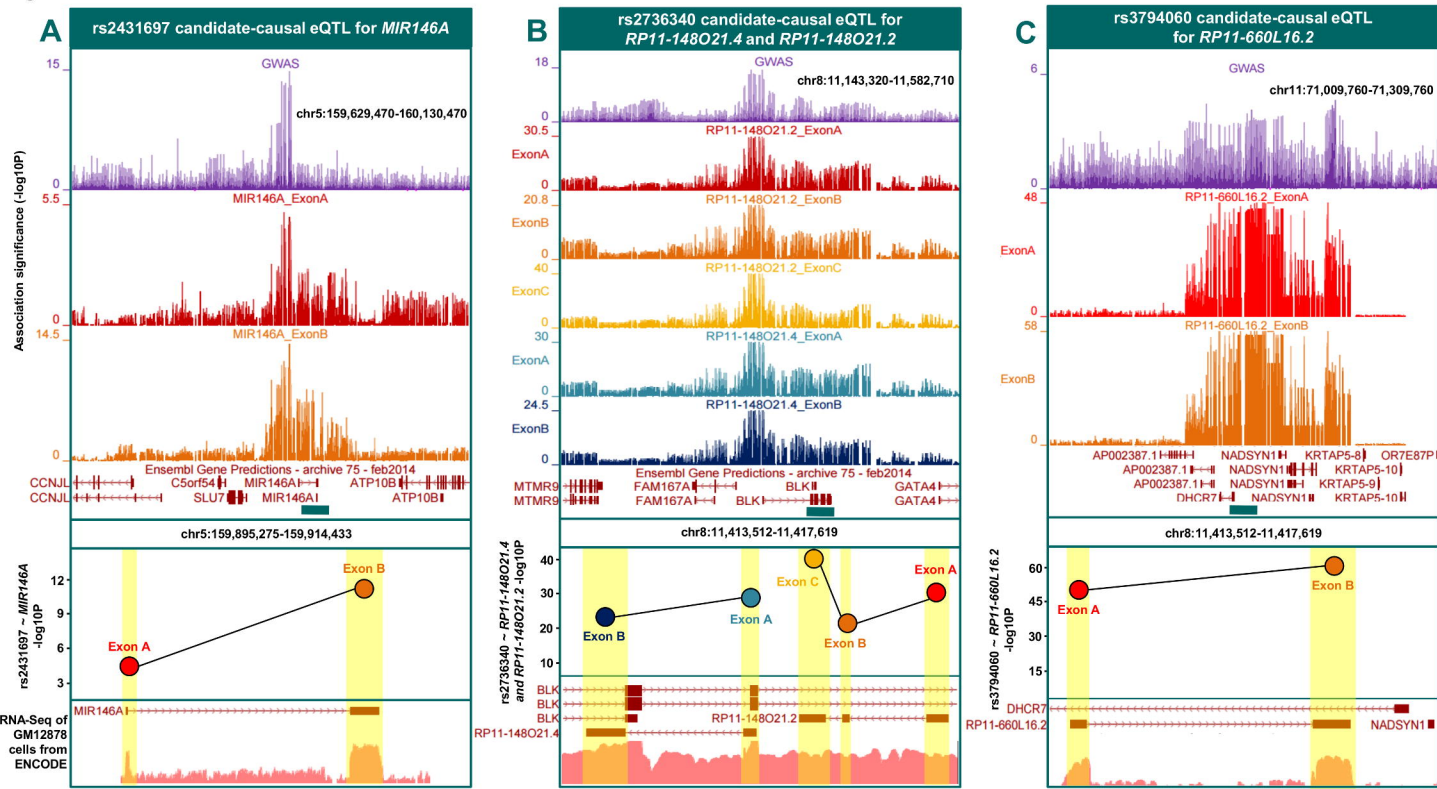
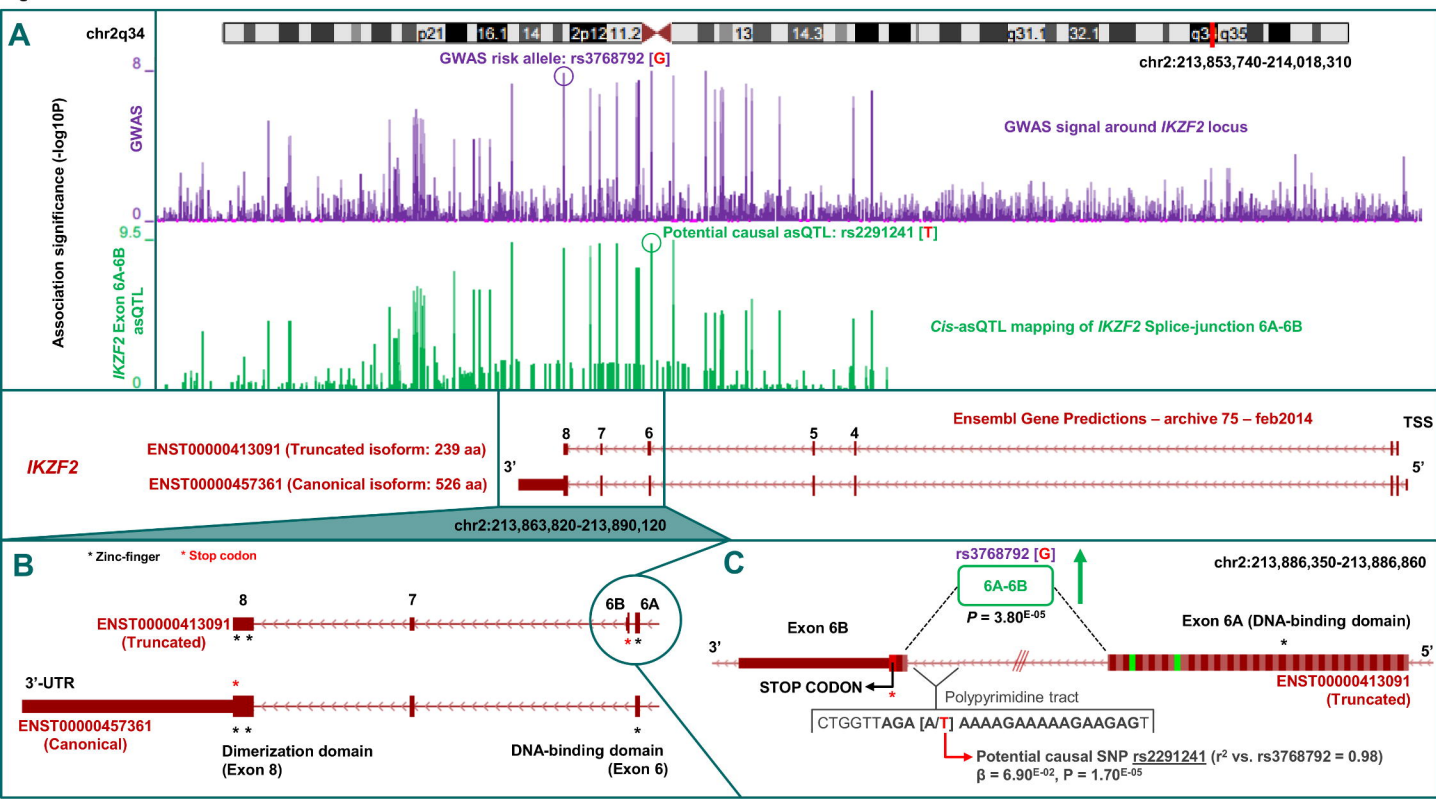


Fig 5.



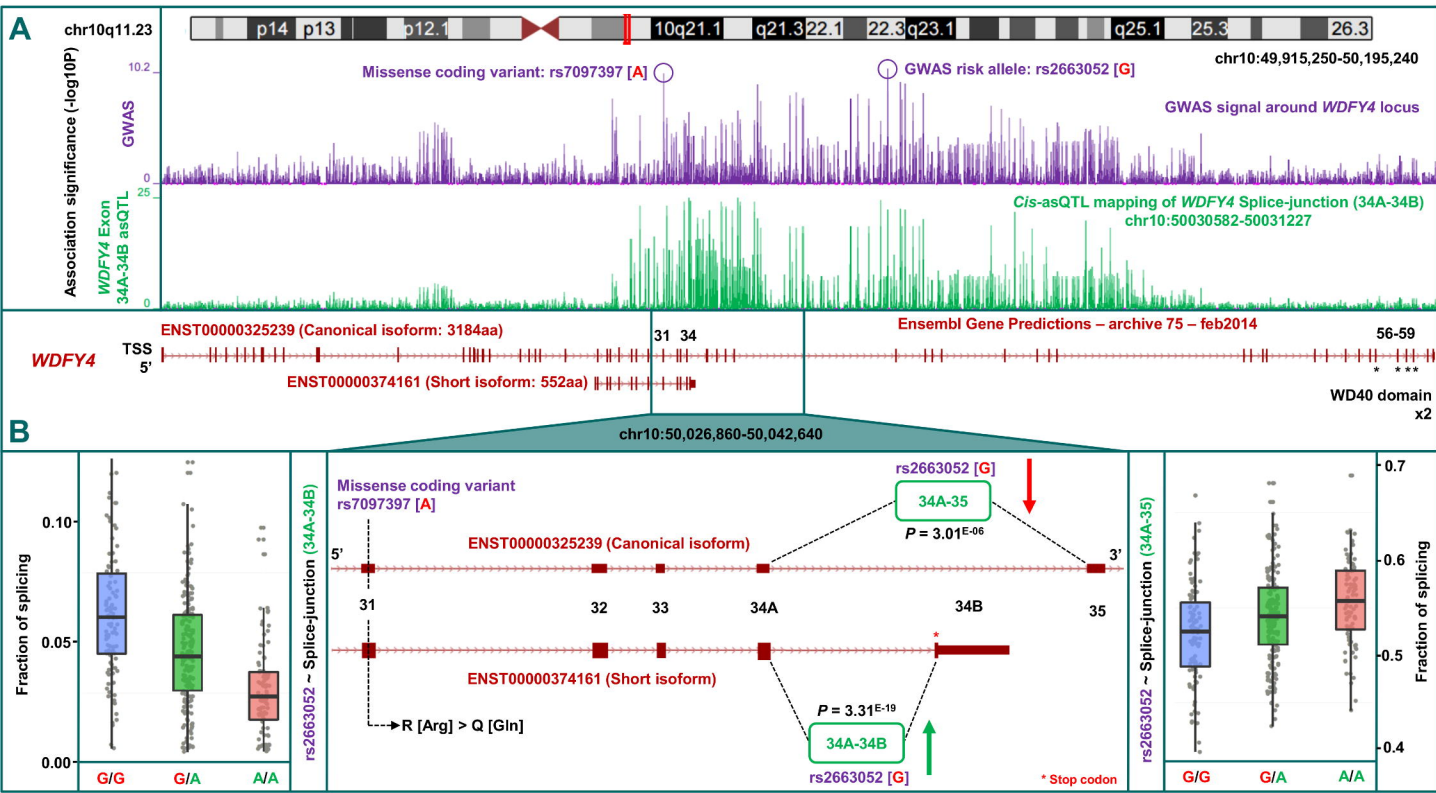


Fig 7.

Relative significance across cohorts

